VARIABILITY OF ATMOSPHERIC AND OCEANIC PARAMETERS USING IRS-P4 OCM DATA

A Thesis Submitted
In Partial Fulfillment of the Requirements
For the Degree of

MASTER OF TECHNOLOGY

by

SAGNIK DEY

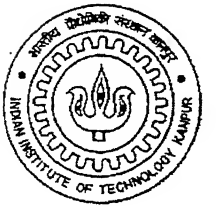

DEPARTMENT OF CIVIL ENGINEERING
INDIAN INSTITUTE OF TECHNOLOGY, KANPUR
February, 2002

CERTIFICATE

It is certified that the work contained in the thesis entitled "**VARIABILITY OF ATMOSPHERIC AND OCEANIC PARAMETERS USING IRS-P4 OCM DATA**" by **Sagnik Dey** bearing roll no. **Y010338** has been carried out under my supervision and the work has not been submitted elsewhere for a degree.

RP Singh 22/02/02

Ramesh P. Singh

Professor
Department of Civil Engineering
Indian Institute of Technology
Kanpur - 208016

ABSTRACT

Visible and infrared remote sensing have been proved to be a successful tool for monitoring various atmospheric and oceanic parameters. The IRS-P4 satellite, which was launched in 1999, carries on-board the Ocean Color Monitor (OCM) sensor. OCM with a total of 8 bands with wavelengths ranging from 412-865 nm, has been designed for remote sensing of ocean and atmosphere. In the present study, atmospheric correction has been carried out to retrieve the ocean parameters like chlorophyll concentration and suspended sediment concentration in the Arabian Sea and the Bay of Bengal. From the atmospheric contribution, the aerosol parameters and column water vapor have been computed. Temporal and spatial variability of aerosol optical depth (AOD) and aerosol size distribution have been studied over the Arabian Sea and the Bay of Bengal. AOD shows minimum value during January-February and increases during summer over both the ocean. AOD also decreases away from the coast to the remote ocean. The coastal regions suffer from the turbidity. Especially in the bay regions, retrieval of AOD is very difficult. A new approach has been taken to retrieve AOD over such regions assuming quasi-homogeneous effects for the correction of water-leaving radiance with soil particles at 412 nm. The results show that the data is continuous from the target regions to the surrounding regions. Aerosol size distribution shows 3 types of particles, of which the lowest radius value, is attributed to the background. The highest value is attributed to coastal aerosols, whereas, the moderate size is typical of marine aerosols. The total column water vapor (TCW) shows a systematic pattern, which shows good correlation with the monsoon. The variability of aerosol parameters has been discussed in view of the wind pattern over these regions. The variability of chlorophyll and suspended sediment concentrations have been discussed and compared in the Arabian Sea and the Bay of Bengal. The results discussed in the present thesis show the potentiality of OCM data to study the variability of atmospheric and oceanic parameters for better understanding of ocean-atmosphere interaction.

ACKNOWLEDGEMENTS

I am deeply indebted, first and foremost to my thesis supervisor Professor Ramesh P. Singh for his valuable guidance, providing his research laboratory facilities, constructive and stimulus criticism during every step of my thesis work. It is his whole-hearted support, cooperation and meticulous scientific attitude, which inspired and enabled me in accomplishing this undertaking work. His ever willingness to help me at any moment is beyond comparison. I am sort of word to express my gratitude for the pain he has taken for me.

The relative humidity data was obtained from the NCEP-NCAR (National center for environmental prediction – National center for atmospheric research) climate reanalysis data center, NOAA, USA. The QuickSCAT data (wind speed and wind direction) were obtained from the NASA Physical Oceanography Distributed Active Archive Center (PO.DOAAC) at the Jet Propulsion Laboratory/California Institute of Technology. Thanks to the Space Application Center, ISRO, Ahmedabad for providing OCM data under OCEANSAT AO project to Professor Ramesh P. Singh. The part of the work is supported through a grant under ISRO-GBP program to Professor Ramesh P. Singh.

I am very much thankful to Deepak Ranjan Mishra and Rahul Kanwar for helping me in QuikSCAT data processing.

My acknowledgement can not be complete without my friends with whom I shared the lab: Alok Sahoo, Sanjeeb Bhoi, Netramani Harijan, Ujjwal, Stefen, Stefan, and Susanna. A special thanks to my friends Jadu, Amlan, Subhobrato, Sonali, Pinaki, Tapas, Bikas, Debobroto and Phalguni for their nice support during my thesis work.

Last but not the least, I thank all the students and members of Engineering Geology Laboratory, Specially Harish Bhai, Dubeyji and all my juniors who were very much cooperative.

Finally, I would like to express my deepest gratitude to family members and Soma, who supported me most throughout my whole academic career. I can hardly pay off their sacrifice. Thanks to all people who have helped me directly or indirectly throughout the project work and have helped me in completing the job successfully.

February 22, 2002 **SAGNIK DEY**

CONTENTS

LIST OF FIGURES

LIST OF TABLES

CHAPTER I

INTRODUCTION

1.0 GENERAL

Accurate and reliable information about the distribution of Earth resources and their monitoring in time and space requires observations at close spacing, which can only be achieved using satellite data. Remote sensing from space has emerged as a very powerful tool for understanding the Earth, its resources and monitoring the environment. Ocean occupies almost 70% of the Earth's surface and greatly affects the global climate as well as influences the economy and life of the people. Also, ocean surrounds India from three sides. So, long-term time series of satellite ocean color measurement are important approach for understanding of the ocean parameters, ocean physical processes and coastal environmental. Monitoring of the atmosphere is also important as the atmosphere, which has direct impact over the population, surrounds the whole Earth.

1.1 OBJECTIVE OF THE PRESENT STUDY

The main objective of the present study is quantitative assessment of the oceanic constituents (e.g. chlorophyll concentration, suspended sediment concentration etc.) from the spectral nature of the solar radiation backscattered from the ocean water. In the broad band electromagnetic spectrum falling on the Earth's surface, only the visible portion (λ= 400 to 700 nm) can penetrate into water. This radiation, after entering into the Sea water, undergoes absorption and multiple scattering by water molecules and water constituents and a very small part is scattered out, which is detected by the ocean color sensor. The concentrations of the oceanic constituents can be estimated from the radiance detected in a set of suitably selected wavelengths, through a retrieval procedure. In the case of space borne ocean color remote sensing, the sensor detected radiance is a mixture of the radiation emerging from the water (water leaving radiance) and the solar radiation backscattered by the air molecules (Rayleigh scattering) and the aerosols (mainly Mie scattering) in the atmosphere. The last two parts of the radiation, called the atmospheric path radiance, is quite strong and constitutes more than 85% of the radiance at the top of the atmosphere (TOA). Therefore, to estimate the oceanic parameters correctly, the atmospheric contribution has to be removed first from the detected radiance. The procedure for removing the

atmospheric contribution from the radiance detected in different channels of the sensor is called atmospheric correction.

In the atmospheric contribution, the most variable constituent is the aerosol. The presence of aerosol over the ocean controls the climate and weather conditions. Over the land, it is possible to deploy a sunphotometer to study the variability of aerosols, on the contrast, it is difficult to measure over the ocean. So, another objective of the present study is to monitor the variability of aerosol parameters. In atmospheric science, the term aerosol is used to designate the particulate suspensions in the atmosphere either in liquid or solid phase. It is an end product, the sink of many complex processes taking place in the atmosphere, the origin of which can also be from a set of gas molecules. Thus, the size range of these particles can vary from a few hundredths of a micrometer- a gas molecule, to a few tens of micrometers- a fine liquid droplet or a sand particle. It was the pioneering work of Junge (1963) that introduced the concept of a dynamic aerosol continuum and paved the way to understand the effects of physical and chemical properties of aerosols on different atmospheric processes. Even today the major challenge in the field of aerosol studies lies in understanding the effects of atmospheric aerosols on atmospheric processes by reconciling them in terms of their physical and chemical properties. The radiative effect of aerosols is felt in a two fold way; one the absorption of solar radiation by these particles and the resultant heating of the ambient atmosphere, thereby affecting the atmospheric processes prevailing in that region and the other by the increased scattering of the solar radiation by these particles causing an increasing in the effective planetary albedo and thereby producing a negative radiative forcing on the Earth's surface.

1.1 ORGANIZATION OF THE THESIS

The present work has been divided into five chapters. In chapter I, introduction, objective of the work have been discussed. Chapter II deals with the basic role of remote sensing and its usefulness in monitoring the ocean and atmosphere. In chapter III, the satellite and sensors used for the present study have been discussed. Chapter IV covers the details of various algorithms used to retrieve different oceanic and atmospheric parameters and the data processing. Detailed results of the present study and the analytical inference have been discussed in chapter V. The summary and conclusions have been discussed in chapter VI.

CHAPTER II

REMOTE SENSING FOR MONITORING OF OCEAN AND ATMOSPHERE

2.0 GENERAL

Remote sensing of ocean and atmosphere is going through a quiet revolution. To understand the magnitude and scope of the revolution, we have to go back to the genesis of ocean-color remote sensing from space. The Coastal Zone Color Scanner (CZCS), the first satellite sensor to monitor ocean color, was launched by NASA in 1978. At that time, the goals of the mission were modest: to measure water-leaving radiance at a limited number of wavebands in the visible domain, and then to use the signal to infer concentrations of pigments in the near-surface layers of the ocean. The algorithms in routine use made the assumption that the atmospheric and the oceanic components of the total signal reaching the sensor could be decoupled using theoretical models of radiative transfer in the atmosphere. Building on the CZCS experience, and learning from theoretical studies and observations from in situ platforms and aircraft, the scope and requirements of remote sensing of ocean color from space have grown drastically over the years.

2.1 INTERACTION OF EM RADIATION WITH THE ATMOSPHERE

All space-borne sensors use some parts of the electromagnetic spectrum, either natural emission from sun or artificial radiation from an object. The sensors which use electromagnetic energy sources of their own are called active sensors, while those, which depend on the solar radiation or natural self-emission are grouped as passive sensors. The electromagnetic radiation (EMR) received and/or transmitted by remote sensing sensors pass through the atmosphere. Thus, the effect of the atmosphere on EMR of various wavelengths or frequencies is very important to measure. As the EMR interacts with the atmosphere, a slight reduction in field strength takes place, except at certain discrete frequencies where EMR is almost totally absorbed. This attenuation of energy is caused by the loss of energy from EMR to the various gaseous constituents, aerosols and water vapors that make up the atmosphere. The amount of attenuation of depends in large part on the frequency of the EMR; in general, higher the frequency, greater is the attenuation. At the higher frequencies,

where the very short wavelengths are almost equal to the mean diameter of the atmospheric particles and molecules (e.g. dust, smoke, haze, CO_2, O_2, water vapor etc.), scattering becomes important.

2.1.1 SCATTERING

When the electromagnetic wave propagates through the atmosphere, two types of scattering, Rayleigh and Mie scattering occur (Ulaby et al., 1981). Rayleigh scattering is caused by a pure or Rayleigh atmosphere consisting purely of gas molecules. Mie scattering is caused by water particles, dust, smoke, industrial byproducts and aerosols. The real atmosphere contains a varying concentration of Mie particles, depending on geographical location, time of day, meteorological conditions and many other factors. Mie particles are largely restricted to lower atmosphere, mostly below 5000 m. Atmosphere is predominantly Rayleigh above 5000 m, and effective Rayleigh scattering ends above 10000 m.

2.1.2 ABSORPTION

There are certain atmospheric constituents, which absorb and reradiate EMR of specific frequencies. The amount of absorption varies with wavelength of radiation. An atmospheric constituent may behave very differently if exposed to radiation of different wavelengths. Because of this absorption, certain single frequency or band in the infrared and microwave portion of the EM spectrum can not be used to obtain remotely sensed data from the Earth's surface and the atmosphere. On the other hand, measurements at these bands provide a great deal of information about the composition and concentration of certain constituents in the Earth's atmosphere. This information is of great value in analyzing remote sensing data, especially of frequencies near the principal absorption bands.

2.1.3 TRANSMISSION

The transmittance of a target or medium is defined as the ratio of radiation at a given level/point to the incident radiation at that very level/point within the medium. The transmission of EMR in relation to absorption and scattering is already discussed above. It is obvious that, in order to conserve energy, the sum of reflection/scattering, absorption and transmission must be equal to the incident energy. Because of the wavelength dependency, the relations between reflection/scattering, absorption and

transmission vary across the EM spectrum. These relationships also depend on angle of incidence, e. g., if the angle of incidence is low, the proportion of reflected energy may exceed sum of absorbed and transmitted energy), whereas, if angle of incidence is high, the transmitted energy may be high.

2.2 MONITORING THE VARIABILITY OF AEROSOLS

The study of marine aerosols provides great importance because of their possible impact on climate through radiative interactions. Marine aerosols play a major role in the formation of clouds in the marine boundary layer, causing changes in the cloud droplet size distribution and hence changes in the cloud albedo, leading to change in radiative coupling between ocean and atmosphere with climatic implications (Charlson et al., 1987; Lawrence, 1993). The spectral extinction of solar radiation passing through the atmosphere depends strongly on the size distribution and refractive index of aerosols. Marine aerosol characteristics are known to be influenced by action of winds (Blanchard and Woodcock, 1980; Monahan et al., 1986). Long range transport of aerosols from the continents (Junge, 1972) and in situ production by photochemical reactions of gaseous emissions by marine phytoplankton (Russell et al., 1994) and thus show temporal and spatial variations.

Atmospheric aerosols, produced as a result of various natural and anthropogenic processes on the earth's surface, are essentially polydisperse, having sizes ranging from one thousandth of a micrometer to a few tens of micrometers. Ocean forms the major sources for natural aerosols. Sea-spray particles produced on the ocean surfaces carry Sea-salt and bacteria from the Seawater. In addition to these continuous sources, events like submarine volcanism and oil fires also dump a lot of gases and particulate matter into the atmosphere. As these particles and gases are carried to higher altitude in the atmosphere, their effects are felt on a global scale.

In recent years, several attempts have been made to assess the impact of aerosols on weather and climate with the help of numerical models. Some of these studies have indicated that on a global scale, aerosols, through their albedo effect, offset the greenhouse forcing by about 20-40 %. Whereas, on a regional scale, they are found to cool the North Atlantic atmosphere, reduce the vertical mixing in the tropical atmosphere, narrow down the ITCZ (Inter Tropical Convergence Zone) and weaken the trade winds and the monsoon by reducing the land-sea temperature contrast. There is a strong effect of aerosols on the vertical temperature profile, when the optical

thickness of the aerosol is large; and a weak effect, if the optical thickness is below 0.5. Depending on surface albedo, optical properties of aerosol and aerosol spatial distribution, both cooling and warming of climate take place. An assessment of the effect of the background aerosol in the troposphere on the radiative regime shows that the aerosol can determine a decrease in the short-wave radiation budget at surface level by an order of 5.0 W/m^2 and at the top of the atmosphere by 3.5 W/m^2. In contrast to the global comparative homogeneity of radiative disturbance due to gases, a specific feature effect on the radiative regime is its spatial inhomogeneity connected with the spatial variability of the aerosol content and surface albedo as well as with variations in the sun elevation. However, there is no total concurrence in the conclusions of different studies made with the numerical models, mainly due to lack of detailed knowledge of aerosol spatial distribution, optical properties, sources and sinks, vertical profile, residence time, transport processes etc.

Satellites, with their capability for large area coverage and short term repetitive, are the most ideal means for acquiring global information on aerosols. Ocean color sensing satellites like IRS P3, IRS P4-OCM and Sea WiFS, though primarily meant for ocean color monitoring, can also detect aerosols over the ocean at frequent intervals. The main objective of these satellites is to monitor the ocean color data from the solar radiation reflected from seawater. But since the radiation coming from water (water leaving radiance) gets mixed with a large amount of solar backscattered radiation produced by the atmospheric constituents and aerosols, this atmospheric contribution has to be removed from the detected radiance for deriving the correct information on the oceanic parameters. This atmospheric contribution is thus noise for retrieval of oceanic parameters. But, while considering the study of the atmosphere, this part acts as signal. In order to do so, OCM is equipped with the additional band of wavelength greater than 700 nm, where no radiation originates from the water because of high infrared absorption and so, all the received radiance is only due to the atmospheric backscatter. Thus, using the band 7 (765 nm) and band 8 (865 nm) of OCM, the variability of aerosol parameters are observed in the present study. It is found that in the bay region, where the turbidity is very high, the aerosol optical depth is often overestimated. In this region, a different approach has been taken for monitoring the variability of aerosols.

2.3 INTERACTION OF ELECTROMAGNETIC RADIATION WITH OCEAN SURFACE

When EMR fall on ocean surface, two kinds of general interaction take place. (1) reflection/scattering of EMR and (2) penetration or absorption of EMR. For a calm Sea surface, specular reflection may occur, however for rough Sea surface with undulations almost of the same order as that of the incident wavelength and Bragg scattering occur. The penetration of EMR into Seawater has been studied extensively. The skin depth (distance through which the incoming wave is attenuated 1/e from its original value), at 3 GHz (λ = 10 cm) is 1 cm, and at blue-green portion the EMS it is 10 - 30 m. Thus, remote sensors for the ocean observations are restricted by their ability to view only surface or near surface features. Seawater is optically very similar to the distilled water. However, in coastal waters the attenuation increases rapidly and the region of maximum energy penetration shifts from blue to green. The reflectance of water varies with wavelength, e. g., in visible band, it is 0.02, whereas, in microwave it is 0.64.

The anisotropy of a phenomenon called capillary waves is responsible for observed dependence of radar backscattering on wind direction. The radar return is generally higher than that of the crosswind. Also the modulation of capillary waves by the underlying gravity waves cause the upwind return generally higher than downwind return. The emissivity of the Seawater depends upon wavelength and polarization and also on the angle of incidence, in microwave frequency range, the emissivity is 0.4. The emissivity and polarization also depends upon surface roughness. Emissivity increases with surface roughness but polarization decreases. There are mainly three mechanisms responsible for variation in emissivity- (1) the tilt effect- this happens when the wavelength of the waves in the ocean is greater than the wavelength of the radiation. The resulting change in the local angles, also causes mixing of polarization state, (2) Sea foam- there is drastic change in the Sea surface emissivity in the presence of air bubbles on the surface and (3) diffraction- this is due to small waves on the surface with wavelength smaller than that of observed radiation.

2.3 OPTICAL OCEAN REMOTE SENSING

The color of the ocean is determined by the interactions of incident light with the constituents present in the water. The significant among them are inorganic particulate

i.e. suspended sediment and free-floating photosynthetic organisms i.e. chlorophyll containing phytoplankton, which absorbs light at blue and red wavelengths and transmit in the green. Particulate matter can reflect and absorb light, which reduces the visibility through the water. Substances dissolved in the water can also affect the color of water. Accurate measurements of light intensity at visible wavelengths produce ocean color data. As ocean color data are related to the constituents present, it is therefore used to monitor the level of biological activity and presence of materials in the ocean water. Ocean color monitor from satellite provides an oceanographic viewpoint that is impossible from ship or shore giving a global scenario. In ocean color analysis, it is normal to distinguish Case 1 water, in which the surface reflectance is dominated by photosynthetically active pigments, from Case 2 water, in which the reflectance is mostly contributed by suspended sediments and dissolved organic matter. Case 2 water is usually, though not always, coastal. Retrieval algorithms for Case 1 water generally assume that the surface concentration of chlorophyll is given by some empirical functions of the upwelling reflectance at the water surface, measured at two or three spectral bands.

In the ocean, light reflects from particulate matter suspended in the water, and absorption is primarily due to the photosynthetic pigments (chlorophyll) present in phytoplankton. The light reflected from these optical interactions on the ocean surface gives the net water-leaving radiance. Radiometers are instruments that measure the radiance intensity at a given wavelength. The measured radiance is quantitatively related to various constituents in the water column that interact with visible light.

CHAPTER III

SATELLITE, SENSOR AND DATA PROCESSING

3.0 GENERAL

Remote sensing sensors operating in the visible and near infrared (VIS/NIR) region are now common tools for monitoring ocean and atmosphere. Sensing at different wavelengths of the electromagnetic spectrum. the sensors allow the transfer of measured data into spectral characteristics of the surface to retrieve different surface parameters precisely and accurately. In the present work, optical data has been used to study the variability of atmospheric and oceanic parameters. The present chapter discusses the optical sensors and the processing of the data.

3.1 IRS P4

IRS P4 is one of the series of Indian Remote Sensing satellites launched by Indian Space Research Organization (ISRO) on May 26, 1999. It has two different payloads, Ocean Color Monitor (OCM) and Multi-frequency Scanning Microwave Radiometer (MSMR) serving in optical and microwave frequencies respectively. The OCM data is very useful for retrieval of oceanic parameters and also its additional two bands at NIR wavelengths are useful in estimating atmospheric parameters (mainly aerosol). Table 3.1 gives in details the orbit characteristics of IRS P4.

Orbits/Cycle	29 days
Cycle duration	2 days
No. of orbits per day	14.5
Mean Altitude	720 km
Semi Major Axis	7098.096 km
Inclination	98.28 degree
Mean Eccentricity	0.00113
Nodal Period	99.31 min
Distance between adjacent traces	1382 km
Distance between successive ground traces	2764 km
Average ground track velocity	6.78 km/s

Table 3.1 IRS P4 orbit characteristics (IRS P4 Handbook, 1999)

3.2 OCEAN COLOR MONITOR (OCM)

OCM has 8 channel sensors operating in visible and near infrared wavelengths. The total upwelling radiation from the ocean surface is weak, so the data handling system with high quantisation resolution is required to take care of the total dynamic range of the signal from land and ocean. OCM optics is based on one lens per band concept. The field of view (FOV) of OCM sensor is $\pm 43^0$ providing a swath of 1420 km from 720 km altitude, for which it has a complex lens design known as 'telecentric'. Table 3.2 gives an insight on the OCM payload characteristics. Eight bands of OCM have different applications. Table 3.3 depicts the application of different spectral bands.

Swath	1420 km	
Ground Resolution		
Along track	236 m	
Across track	360 m	
Radiometric Resolution	12 bits	
Spectral Bands	8	
Camera MTF (at Nyquist frequency)	> 0.2	
SNR (at maximum saturation radiance)	> 512	
Spectral characteristics	Range (nm)	Saturation Radiance
		Ocean / Maximum
Band 1	402 – 422	12.5 / 53.0
Band 2	433 – 453	11.7 / 58.5
Band 3	480 – 500	10.3 / 67.3
Band 4	500 – 520	10.1 / 58.6
Band 5	545 – 565	9.1 / 56.7
Band 6	660 – 680	7.7 / 49.5
Band 7	745 – 785	5.2 / 40.7
Band8	845 – 885	6.3 / 31.1

Table 3.2 OCM Payload characteristics (IRS P4 Handbook, 1999)

Band No.	Band Center (nm)	Band Width (nm)	Applications
1	412	20	Yellow substance and turbidity
2	443	20	Chlorophyll absorption maximum
3	490	20	Chlorophyll and other pigments
4	510	20	Turbidity and suspended sediment
5	555	20	Chlorophyll and suspended sediment
6	670	20	Chlorophyll absorption
7	765	40	Oxygen absorption R-branch, Aerosol optical thickness
8	865	40	Aerosol optical thickness, vegetation, water vapor, reference over the ocean

Table 3.3 Details of OCM sensors and applications (IRS P4 Handbook, 1999)

3.3 DATA PROCESSING

The IRS P4 OCM data are provided by National Remote Sensing Agency (NRSA), Hyderabad. The data cover the region (1) bound by 65.84 E longitude to 79.49 E longitude and 31.29 N latitude to 16.76 N latitude and region (2) bound by 75.82 E longitude to 89.67 E longitude and 19.34 N latitude to 5.08 N latitude. Region 1 depicts northern part of the Arabian Sea along western part of India. In the present work the data of January 2, 2000; February 29, 2000; March 2, 2000 and April 29, 2000 from Arabian Sea have been used. Region 2 covers southern part of Bay of Bengal and southeastern part of India. In the present work, the data of November 16, 1999; December 10, 1999; January 21, 2000; February 3, 2000; March 21, 2000 and May 28, 2000 from Bay of Bengal have been used. The IRS P4 OCM raw data of unsigned 16-bit format have been used for the purpose. The OCM data in 8 bands have been imported using ERDAS 8.3.1 and images have been displayed in 8 bands. These images are georeferenced by taking suitable ground control points with the help of a standard map of the concerned area. Then atmospheric parameters have been calculated from the band 7 and 8 of OCM data. The land portion has been masked. The atmospheric correction has been applied on OCM data before retrieving ocean

parameters. Fig. 3.1 shows the steps in sequence needed for the atmospheric correction.

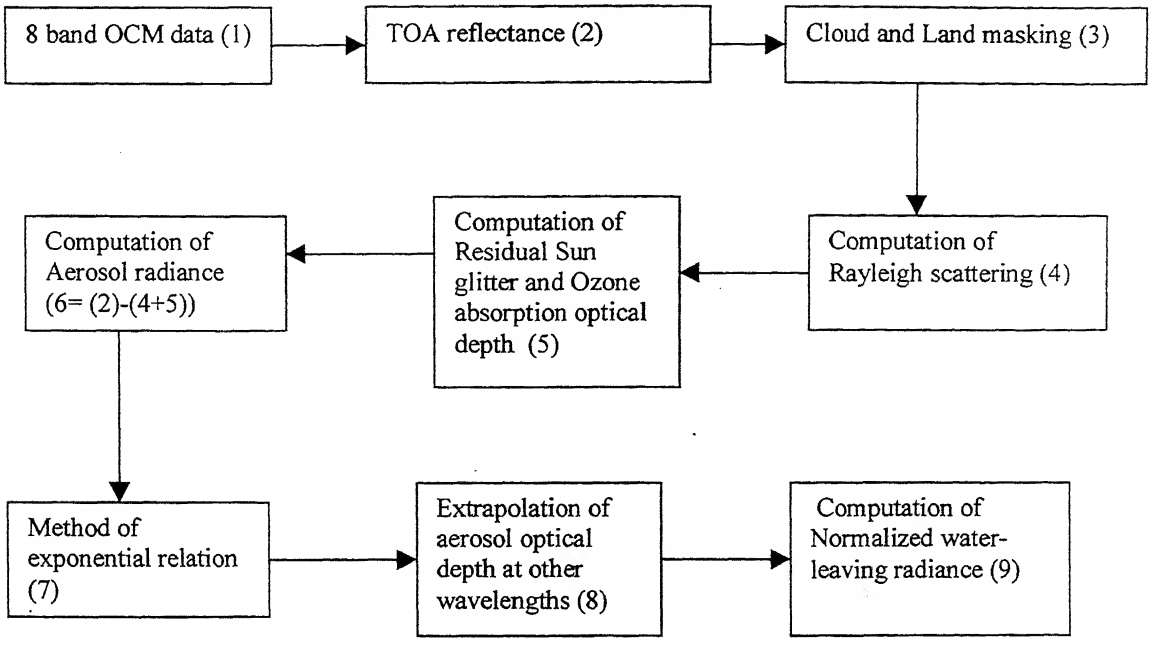

Fig. 3.1 Flow chart of the atmospheric correction

The atmospheric correction is necessary for enhancement of the subdued oceanic features. First, Rayleigh radiance has been computed. Then aerosol radiance has been calculated using the spectral nature of water in the near-infrared wavelengths. Finally, the Rayleigh and aerosol radiance has been subtracted from the TOA radiance to obtain only the water-leaving radiance. The variability of aerosol parameters and the water vapor content have been calculated over both the Arabian Sea and the Bay of Bengal. Chlorophyll concentration and suspended sediment concentration have been computed.

CHAPTER IV

ALGORITHMS USED FOR RETRIEVAL OF ATMOSPHERIC AND OCEANIC PARAMETERS

4.0 GENERAL

India is surrounded by ocean from three sides. The ocean-atmosphere interaction has significant impact on the climate of India and also on the coastal region. The retrieval of the atmospheric and oceanic parameters is very important for better understanding of the climatic conditions. This chapter discusses the various algorithms used for retrieval of some of the atmospheric and oceanic parameters

4.1 AEROSOL

The ocean color sensing satellites measure radiance in visible and near infrared wavelengths and indirectly provide information on the atmospheric aerosols (Gordon, 1997). The radiance detected by a spaceborne sensor at the top of the atmosphere (TOA) in the wavelength (λ) can be split into four terms (Doerffer, 1992):

$$L_t(\lambda) = L_a(\lambda) + L_r(\lambda) + t_d(\lambda) \, . \, L_w(\lambda) \quad \ldots\ldots\ldots\ldots\ldots \quad 4.1.1$$

where,

L_t = sensor detected radiance,

L_a = aerosol path radiance = $F_o \, . \, \omega_{oa} \, . \, \tau_a \, . \, p_a \, / \, (4\pi \cos \theta_v)$ 4.1.2

L_r = Rayleigh path radiance = $F_o \, . \, \omega_{or} \, . \, \tau_r \, . \, p_r \, / \, (4\pi \cos \theta_v)$ 4.1.3

L_w = water leaving radiance,

ω_{oa} = aerosol scattering albedo,

ω_{or} = Rayleigh single scattering albedo ,

θ_v = satellite viewing zenith angle,

$\tau_{a,r}$ = aerosol/Rayleigh optical depth,

$p_{a,r}$ = aerosol/Rayleigh scattering phase function,,

$t_d = \exp [- (1/\cos \theta_v + 1/\cos \theta_s) (\tau_r/2+\tau_{oz})]$ = atmospheric diffuse transmittance,

θ_s = solar zenith angle and

τ_{oz} = ozone absorption optical depth

In equation 4.1.1, the Rayleigh and aerosol path radiance together constitutes the atmospheric path radiance. The phase function $p_{a,r}$ depends on the Fresnel reflectance

of the water surface and the scattering angle. In order to obtain the water leaving radiance, the aerosol and Rayleigh path radiance have to be removed from the TOA radiance (L_t) and has to be divided by t_d. The Rayleigh path radiance is computed, as the spectral dependence of the Rayleigh optical depth and the Rayleigh phase function are well known. The diffuse transmittance is also calculated from the Rayleigh optical depth and ozone absorption optical depth. The value of the ozone absorption optical depth is taken nearly constant, since its variation within the spectral range of ocean color sensor is negligible.

The aerosol path radiance is difficult to determine, as the aerosol parameters are highly variable, both spatially and temporally. But, making use of the wavelengths above 700 nm, it is possible to determine the aerosol path radiance indirectly. In the spectrum of the sensor of OCM, there will be no water leaving radiance for wavelengths above 700 nm, due to strong infrared absorption by water. The detected TOA radiance is just the sum of the aerosol path radiance and Rayleigh path radiance. The aerosol path radiance is calculated from the TOA radiance at 765 and 865 nm wavelengths knowing the value of Rayleigh radiance at these wavelengths. Then the aerosol path radiance is computed for the other bands of the OCM, through extrapolation method (Gordon, 1997).

4.1.1 AEROSOL OPTICAL DEPTH

The aerosol optical depth is calculated at 765 nm and 865 nm wavelengths using the equation 4.1.1 and 4.1.2

$$\tau_a = (L_t - L_r) / [F_o / (p_a \cdot 4\pi \cos \theta_v) \quad \ldots\ldots\ldots\ldots\ldots \quad 4.1.4$$

4.1.2 THE METHOD OF EXPONENTIAL RELATION

The aerosol optical depth is assumed to have an exponential relationship with the wavelength. Considering the aerosol phase function to remain constant over the ocean color wavelength range, one can write (Gordon, 1997)

$$L_a / F_o = \text{constant} \cdot \exp(-c \cdot \lambda) \quad \ldots\ldots\ldots\ldots \quad 4.1.5$$

where c is a constant. Taking the log of both sides, c is determined as the negative slope of the straight line as

$$c = [\log (L_{a1} / F_{o1}) - \log (L_{a2} / F_{o2})] / (\lambda_2 - \lambda_1) \quad \ldots\ldots\ldots \quad 4.1.6$$

Once c is known, the aerosol path radiance for the wavelengths below 700 nm is determined as (Gordon, 1997)

$$L_a (\lambda < 700 \text{ nm}) = L_{a1} . (F_o / F_{o1}) . \exp [-c . (\lambda/\lambda_1)] \ldots\ldots \quad 4.1.7$$

Then water-leaving radiance is calculated using equations 4.1.1

$$L_w = [L_t - L_r - L_a] / t_d \ldots\ldots \quad 4.1.8$$

4.1.3 ALGORITHM FOR CORRECTING THE EFFECT OF TURBIDITY

The coastal region, especially bay region suffers from the turbidity and therefore the retrieval of aerosol optical thickness over there is difficult. Aerosol retrieval in near infrared wavelengths incorporates only the contribution of atmospheric particles. However, if the water contains soil particles, the radiance in near infrared region fluctuates largely and the radiance pattern only form the aerosol contribution becomes undetectable. The algorithm for retrieval of aerosol parameters over such region should be treated in a different way. Recently, Okada et al. (2001) have proposed an algorithm, where the ratio of radiance at 412 nm wavelength to 443 nm wavelength is taken for the near coastal region. If there is substance, which absorbs largely at 412 nm and absorbs less at 443 nm, the ratio becomes less (in near coastal region) On the other hand, in other region, where the water contains substances absorbing less at 412 nm and more at 443 nm wavelengths, the ratio become large. The value of 1.1 is considered to be the threshold value to distinguish between these two regions. For fixing the threshold, the following assumptions are have been made; (1) contribution from the atmosphere has large variations and (2) contribution of water substances with soil particles show quasi-homogeneous effects at 412 nm. For the retrieval of aerosol optical depth, the following steps are followed:

- The ratio of radiance at 412 nm to 443 nm is taken (to distinguish between the regions)
- The Rayleigh correction has been done on the TOA radiance given by OCM data
- The threshold value is subtracted from the Rayleigh corrected radiance value to exclude the contribution of the turbid water with soil.
- The aerosol optical depth at 412 nm wavelength has been retrieved from the Rayleigh and soil-water corrected radiance.
- The aerosol optical depth is determined at 765 nm wavelength to study the

contribution of the turbid water.

4.1.4 AEROSOL SIZE DISTRIBUTION

The aerosol size distribution is usually represented in three different ways depending on the physical aspect of interest. The number size distribution represents the number density of the particles for a given radius for unit radius interval. From the standpoint of surface chemistry and optical effects, the surface area distribution is of great interest and for the study of chemical mass balance and physiological effects, the volume or the mass distribution is of great interest.

Using aerosol optical depths at different wavelengths, the columnar size distribution function of aerosols has been retrieved by numerical inversion of the integral equation (Moorthy et al., 1990))

$$\tau_p(\lambda) = \int \pi r^2 Q_{ext} n_c \, dr \quad \ldots\ldots\ldots\ldots \quad 4.1.7$$

where r is the particle radius, Q_{ext} is the Mie extinction efficiency parameter, τ_p is the aerosol optical depth at wavelength λ and n_c is the columnar size distribution of aerosols. The column size distribution of aerosol is given by (Moorthy et al., 1990)

$$n_c \, dr = \int n(r) \, dr \quad \ldots\ldots\ldots\ldots \quad 4.1.8$$

where n (r) dr is the number of particles in unit volume of atmosphere in a size range (dr) centered at r. There are different forms of analytical functions to represent the aerosol number size distribution (Deepak and Box, 1981). Of these, the power law type distribution is the simplest and widely used size distribution to represent the natural aerosol system. The size of the aerosol particles varies by orders of magnitude it will be convenient to represent the distribution in terms of log power law distribution, which is given by (Deepak and Box, 1981)

$$n(r) = 0.434 \, r^{-v} \quad \ldots\ldots\ldots\ldots \quad 4.1.9$$

where v is the aerosol angstrom component. This type of distribution assumes the constant number density from 20 nm to 100 nm and then decrease with increase in particle radius. As far as optical effect is concerned this form of the size distribution can represent the general features of aerosol scattering.

4.1.5 AEROSOL RESIDENCE TIME

The residence time of the aerosol particles depends on the particle size. The lifetime varies from few hours near the surface to few years at higher altitude (in the

stratosphere). Estimation of the aerosol residence time is quite difficult because of the involved complex dynamic processes. Over the ocean, the residence time of the aerosol particles is deduced from the formula given by Jaenicke 1984. At intermediate sizes (radius 0.1 to 10 μm), the residence time increases sharply as the efficiency of sedimentation and diffusive processes decrease, and is mostly determined by wet removal process. The form can be represented by

$$1/T = 1/C \,.\, (r/R)^2 + 1/C \,.\, (r/R)^{-2} + 1/T_{wet} \quad \ldots\ldots\ldots\ldots \quad 4.1.10$$

where T is the residence time (in sec), r is the particle radius, R is the normalization radius (0.3μm), C is a constant ($1.28 * 10^8$ s) and T_{wet} is residence time ($6.91 * 10^5$ s) resulting from wet removal processes.

4.2 COLUMN WATER VAPOR

Atmospheric water vapor has a great impact on the climate of the earth. The column water vapor content over ocean region can be derived from space borne microwave sensor data (Schlussel and Emery, 1990). SSM/I data has been proved to be very successful in quantifying the column water vapor in the atmosphere. In the present study, an attempt has been made to retrieve column water vapor by using IRS P4 OCM data.

TCW gives the total column water vapor present in the atmosphere at a particular time. For better comparison of the data derived from the OCM sensor with the data derived by using microwave sensor, the column water vapor is represented in mm. scale. In the present work, the algorithm, described below, to deduce the column water vapor is taken from Bennartz et al. (1998).

- First, Continuum Interpolated Band Ratio (CIBR) is calculated as:

  $$CIBR = L(\lambda_v) / c_1 L(\lambda_{w1}) + c_2 L(\lambda_{w2}) \quad \ldots\ldots\ldots\ldots \quad 4.2.1$$

  where L is the radiance at the top of the atmosphere. The index v indicates the water vapor channel and w_1 and w_2 are the two neighboring window channels. The coefficient c_1 and c_2 are defined as:

  $$c_1 = (\lambda_{w2} - \lambda_v) / (\lambda_{w2} - \lambda_{w1}) \text{ and } c_2 = (\lambda_v - \lambda_{w1}) / (\lambda_{w2} - \lambda_{w1}) \quad \ldots\ldots\ldots 4.2.2$$

- The 765 nm band is the most sensitive to variations in atmospheric water vapor content and correspondingly the 670 nm and 865 nm bands are selected for the window channels.
- The water vapor path value (V_p) is determined from the equation given by Tahl

and Schonermark (1998) :

$$V_p = (\ln (CIBR) / 0.592)^{1/0.568} \quad \text{(for ocean)} \quad \ldots\ldots\ldots 4.2.3$$

$$V_p = (\ln (CIBR) / 0.599)^{1/0.575} \quad \text{(for land)} \quad \ldots\ldots\ldots 4.2.4$$

- Taking radiation at the top of the atmosphere, the portion of the path radiance compared to the reflected radiance is larger over the low radiating surfaces. As the path radiance does not reach the Earth's surface, it has a shorter way through the atmosphere than the surface reflected radiance and therefore it has less penetration through the water vapor. Therefore, to correct the underestimation of water vapor content for low reflecting surface the correction factor given by Tahl and Schonermark (1998) for ocean and land has been taken as:

$$V_{p,corr} = V_p / 0.464 + 0.130 * \ln [c_1 L (670) + c_2 L (865) / \cos \theta_s] \ldots\ldots\ldots 4.2.5$$

$$V_{p,corr} = V_p / 0.464 + 0.130 * \ln [c_1 L (670) + c_2 L (865) / \cos \theta_s] \ldots\ldots\ldots 4.2.6$$

- The water vapor path radiance is converted to the column water vapor (Vc) by means of the zenith angle of the sun and sensor according to the equation (Tahl and Schonermark, 1998)

$$V_c = V_p (1 / \cos \theta_v + 1 / \cos \theta_s)^{-1} \quad \ldots\ldots\ldots\ldots 4.2.7$$

4.3 CHLOROPHYLL CONCENTRATION

Numerous bio-optical algorithms for retrieval of chlorophyll concentration have been developed. Most of these algorithms are derived from the statistical regression of water leaving radiance versus chlorophyll concentration. Advances in various theoretical studies and new parameterization of some optical properties have yielded better knowledge. O'Reilly et al. (1998) have proposed an empirical algorithm for Sea WiFS ocean color data. This algorithm captures the inherent sigmoid relationship between R_{rs} 490/R_{rs} 555 band ratio and chlorophyll concentration (C), where R_{rs} is the remote sensing reflectance. This algorithm is found to retrieve low as well as high chlorophyll concentration, which means a better retrieval even in the case of case 2 water. The algorithm operates with 5 coefficients with the following mathematical form (Chauhan et al., 2000)

$$C = 10\text{^}(0.319–2.336 * R + 0.879 * R^2 – 0.135 * R^3) – 0.071 \ldots\ldots 4.3.1$$

for 0.01 mg/m^3 <= C <= 50 mg/m^3, where C is the chlorophyll concentration in mg/m^3 and $R = \log_{10} [R_{rs} (490) / R_{rs} (555)]$. This algorithm is found to be good even

for case 1 water of the Arabian Sea (Chauhan et al., 2000) and so selected for retrieval of chlorophyll concentration in the Arabian Sea as well as the Bay of Bengal.

4.4 SUSPENDED SEDIMENT CONCENTRATION

It has been demonstrated by a large number of studies that remote sensing can be a successful tool in determining the suspended matter concentration in the coastal seas. The study of suspended sediment has an ecological importance because it is the main carrier of the various inorganic and organic substances (including pollutants) and becomes the main substrata for biogeochemical processes. The transport and distribution of the suspended sediment inyo the coastal Sea is attributed to the processes such as tides, waves, ocean and river current and wind stress. Suspended sediment also affects the penetration of light and the transport of nutrients, shoreline morphology and many other processes.

Numerous algorithms have been proposed to quantify suspended sediment using ocean color sensor data. The algorithm described below has been tested to provide the best result in the coastal areas using water leaving radiance derived from OCM data (Tassan and Strum, 1986).

$$S = 25.0 * \exp (2.16 + 0.991 * \log X) \quad \ldots\ldots\ldots\ldots \quad 4.4.1$$

where S is the suspended sediment concentration in mg/l and X is the variable defined as

$$X = [[R_{rs}(555) - R_{rs}(670)] * [R_{rs}(490) / R_{rs}(555)]]^{-1} \quad \ldots\ldots\ldots \quad 4.4.2$$

where R_{rs} is the remote sensing reflectance in respective wavelengths.

CHAPTER V

RESULTS AND DISCUSSION

5.0 GENERAL

In the present chapter IRS-P4 OCM data has been analyzed over the Arabian Sea and the Bay of Bengal and the atmospheric and oceanic parameters have been compared. The aerosol optical depth at wavelengths 765 and 865 nm, aerosol size distributions have been derived over both the ocean. Total column water vapor has been deduced over the ocean. Chlorophyll and suspended sediment concentrations have been retrieved and inter-annual variability of the parameters over the Arabian Sea and the Bay of Bengal have been studied.

5.1 ATMOSPHERIC PARAMETERS

5.1.1 AEROSOL OPTICAL DEPTH

Aerosol optical depth (AOD) has been computed at wavelengths 765 and 865 nm over the Arabian Sea and the Bay of Bengal. Fig. 5.1 shows the spatial distribution of AOD at wavelengths 765 and 865 nm and turbidity-corrected AOD at wavelength 765 nm over the Arabian Sea during January, February, March and April 2000. AOD is seen to be higher near the coastal region compared to the remote ocean. In some of the images, AOD is seen to be high near the clouds, which is attributed to the high radiance of clouds. In January, the AOD over the Arabian Sea and most of the region is found to be greater than 0.15, with the highest value of $\approx$ 0.4 close to the Gulf of Cambay coast. In general, AOD over the Arabian Sea in February is low compared to that in the month of January. Again, it increases in March and reaches to a maximum value of 0.45 near the western coast of India during April. It is also seen that AOD decreases with the wavelengths. The spatial variations of AOD over the Arabian Sea are clearly seen (Fig. 5.1). Along the coast, AOD is found to be higher in the bay region, with the highest value in the Gulf of Cambay during all the seasons. During March, an aerosol plume has been seen in the northwestern part of the Arabian Sea, close to the coast of Pakistan. In general, a higher variation in AOD is observed during summer compared to that during winter (Fig. 5.1).

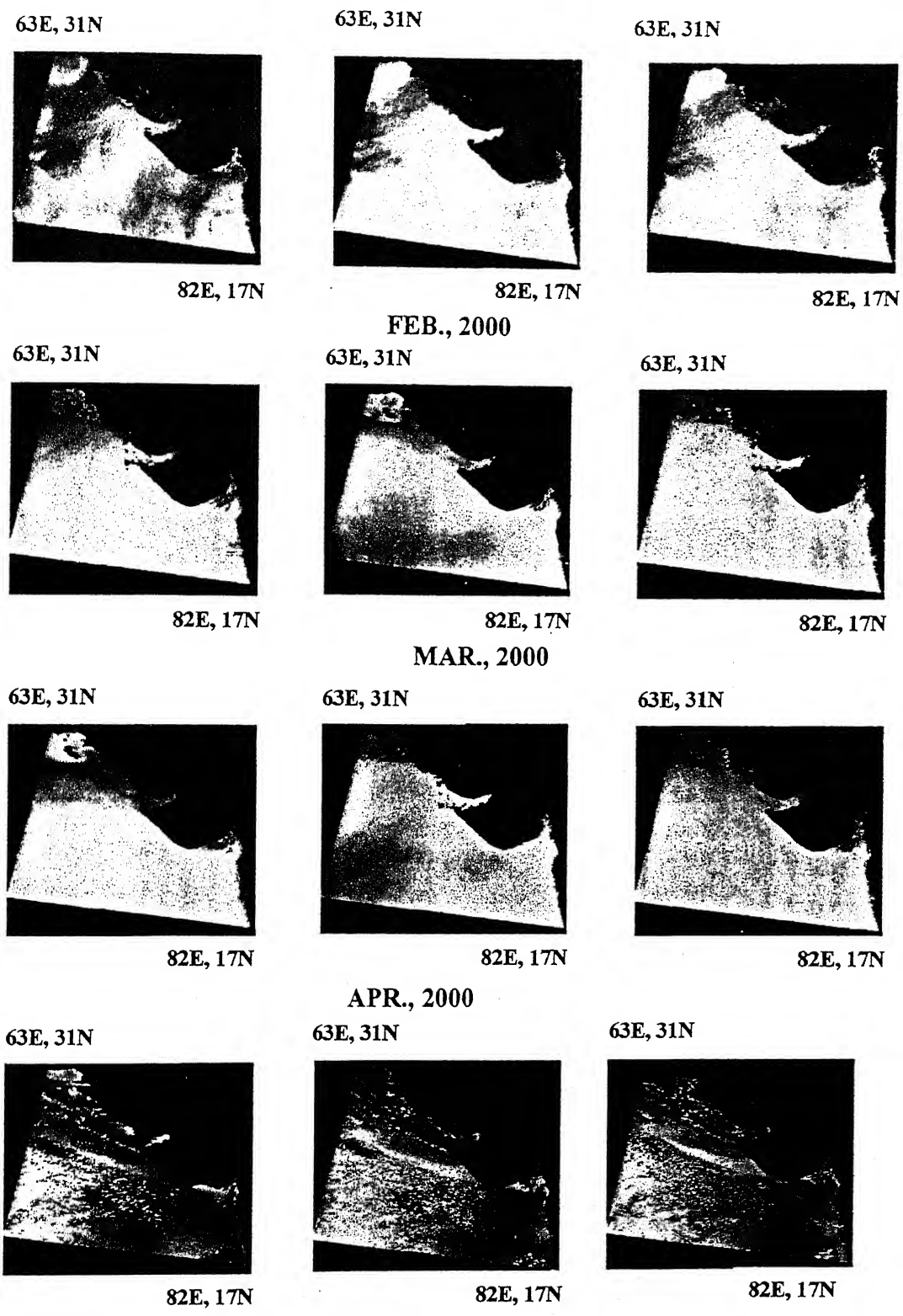

Fig. 5.1 AOD over the Arabian Sea

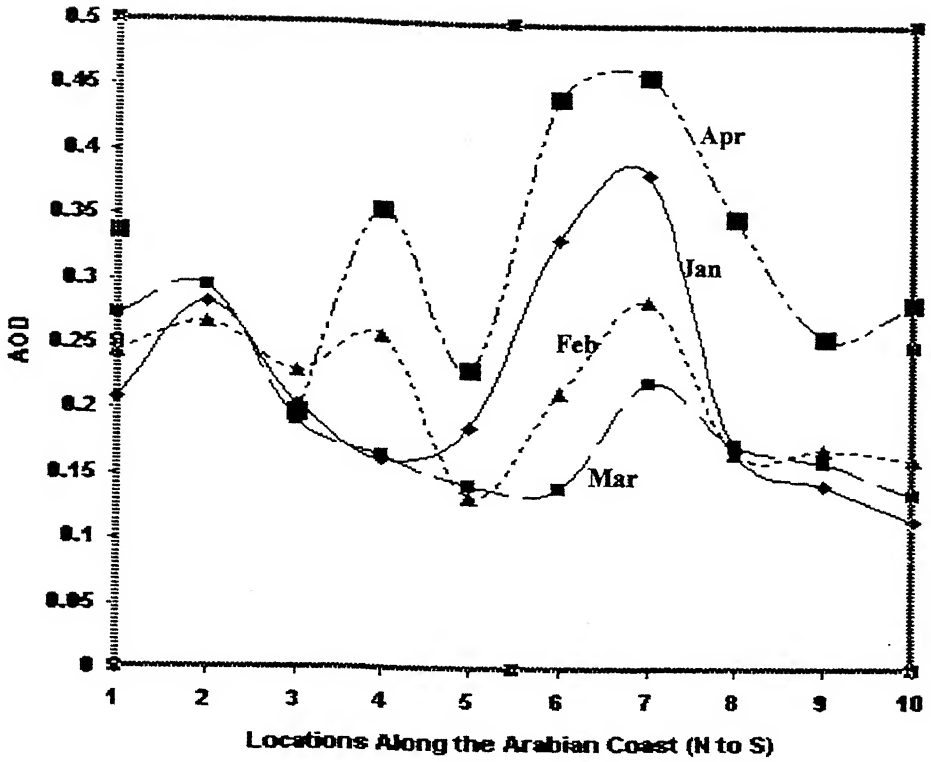

Fig. 5.2 AOD at wavelength 765 nm along the Arabian Sea

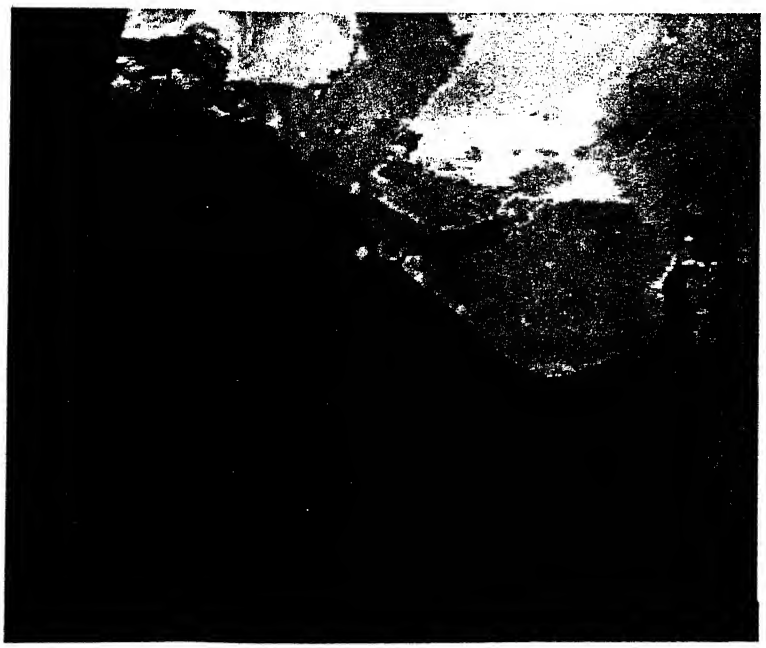

Fig. 5.3 Location of points along the Arabian Sea

Fig. 5.2 shows the AOD over some selected points (Fig. 5.3) along the Arabian Sea coast. The AOD is found to be higher during all months at locations 4 and 7, which are the Gulf of Kutch and the Gulf of Cambay. The high AOD in these regions is attributed to the transport of pollutants from Ahmedabad and Surat City, which are in close vicinity. The transport is aided by wind from land to ocean during January to April (Fig. 5.14). At other locations except 4, 6 and 7, AOD shows very little variation. In the bay region, AOD has been corrected for turbidity. Higher sediment concentrations in these regions cause higher water leaving radiances. This leads to some contribution even in the near-infrared region, which causes overestimation of AOD. The results show that after correcting the effect, AOD in these regions decrease, which is comparable to the other locations. It has been found that higher correction is needed for the month of January, when the suspended sediment is also high. AOD has been found to decrease with the increase in wavelength.

NOV., 1999

DEC., 2000

JAN., 2000

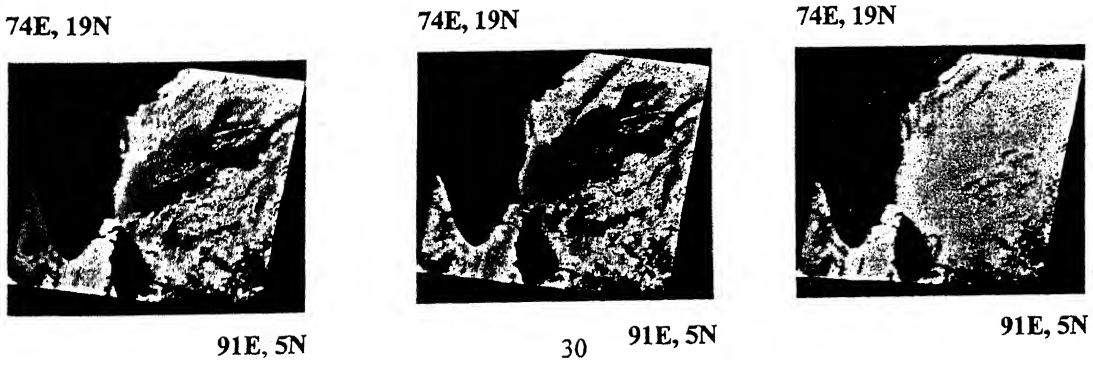

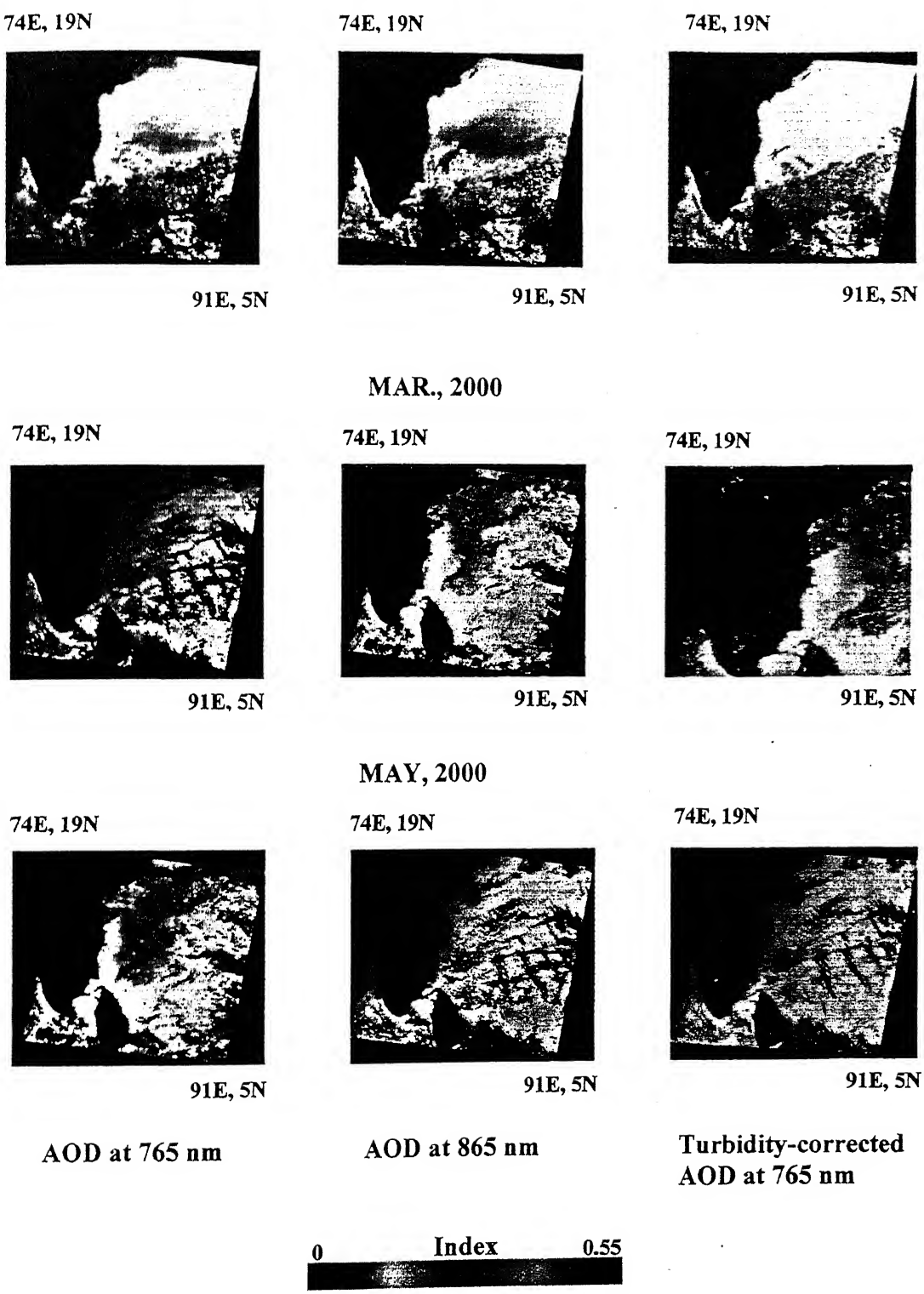

Fig. 5.4 AOD over the Bay of Bengal

Fig. 5.4 shows the AOD at wavelengths 765 and 865 nm and turbidity-corrected AOD at 765 nm over the Bay of Bengal during November, December, 1999; January, February, March and May, 2000. The black patches in the ocean represent cloud cover (Fig. 5.4). Generally, the AOD over the Bay of Bengal is comparable to those over the Arabian Sea. AOD over the Bay of Bengal shows moderate value in November and December 1999, which is found to decrease in January and February 2000. From March onwards, AOD increases, (>0.4) in some regions. Similar to the Arabian Sea, higher values of AOD is seen in the coastal region compared to the remote ocean. AOD value is found to be higher at wavelength 765 nm compared to those at 865 nm. During winter, higher AOD values are seen near the southeastern coastal region and Sri Lanka, whereas, during summer, higher AOD values are seen near the Andhra coast. Northern part of the Indian Ocean surrounded with the Arabian Sea and the Bay of Bengal show higher AOD (>0.4) in the months of November and March. Bay of Bengal is characterized by large spatial gradient of AOD, which decreases rapidly away form the coast. A region of minimum AOD is observed at the central part of the Bay of Bengal during all the Seasons, which shows very small change from winter to summer Season. The effect of turbidity in water on AOD has also been considered. It is seen that the effect is negligible in the remote ocean. The effect is very pronounced in the coastal region, especially the bay region, where the influx of sediments is very high. Fig. 5.5 shows the variations of AOD at wavelength 765 nm along the Bay of Bengal coast.

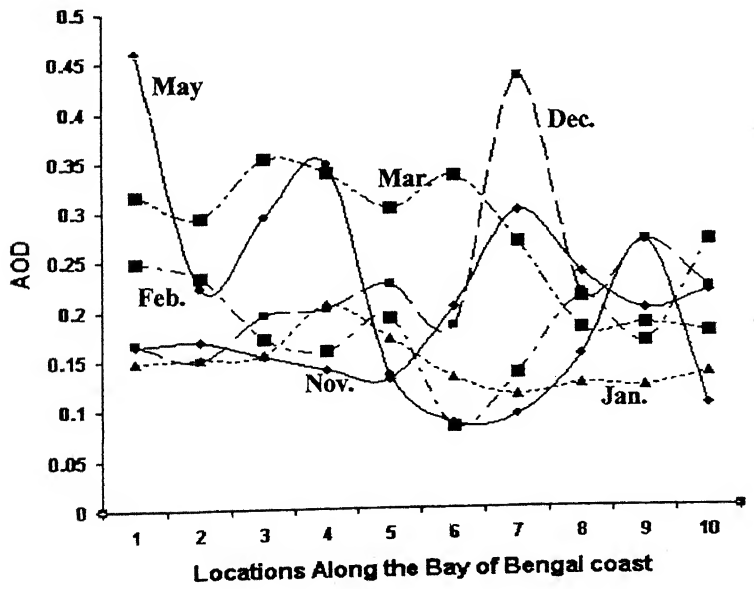

Fig. 5.5 AOD at wavelength 765 nm along the Bay of Bengal

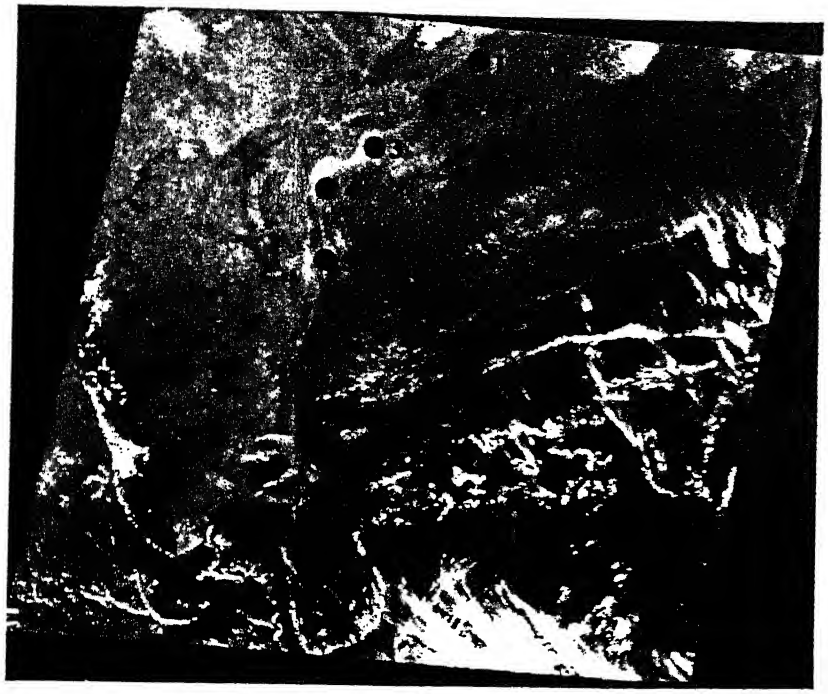

Fig. 5.6 Location of points along the Bay of Bengal

Fig. 5.6 shows the locations along the Bay of Bengal coast. There are no such locations in the Bay of Bengal, over where AOD is higher for all the months. The results show that in general AOD is higher during May, but it varies within the range 0.15 to 0.45. During the month of January, AOD is found to be lower compared to any other month. In February, AOD is lower in most of the locations, but shows abnormally high value in location 7. The turbidity-corrected AOD value in the bay region shows over-estimation of the AOD, which is attributed to the significant water leaving radiance at near-infrared wavelengths.

5.1.2 AEROSOL SIZE DISTRIBUTION

Aerosol size distribution has been studied over the Arabian Sea and the Bay of Bengal. The small particle radius in the range of 0.001 to 0.004 μm is attributed to background aerosol, which is related to air mass characteristics. Over the remote ocean, aerosol particle with 0.1 μm radius is found, which is attributed to Sea-spray aerosols produced by prevailing high wind. Near the coast, aerosol particles are found with radius 2.1 μm, which is attributed to nascent particles produced by a current wind speed. Fig. 5.7 shows variations of the three types of aerosol particles for the months January to April.

shows variations of the three types of aerosol particles for the months January to April.

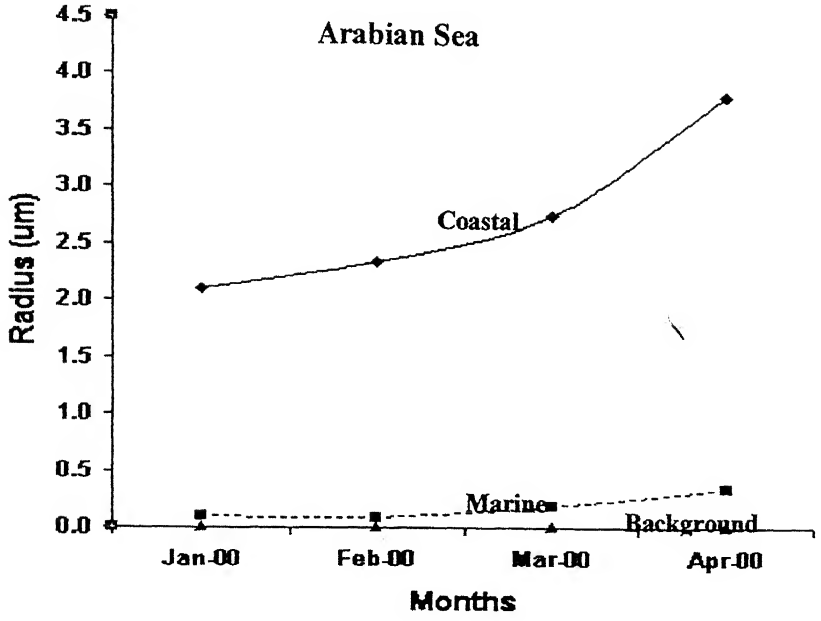

Fig. 5.7 Aerosol particle size over the Arabian Sea

It has been seen that the background particle size remains unchanged, whereas, the other two types of particles increase in size during summer. The variation of the Sea-spray aerosols is much less compared to that of the coastal aerosols. The increase in aerosol particle size is attributed to increase in relative humidity in the atmosphere. With increase in relative humidity, aerosol particles grow in size due to condensation of water vapor from the atmosphere. The growth rate, however, depends on the activity of water on the aerosol particles. Fig. 5.8 shows the effect of relative humidity on the aerosol particle size near the Arabian Sea coast.

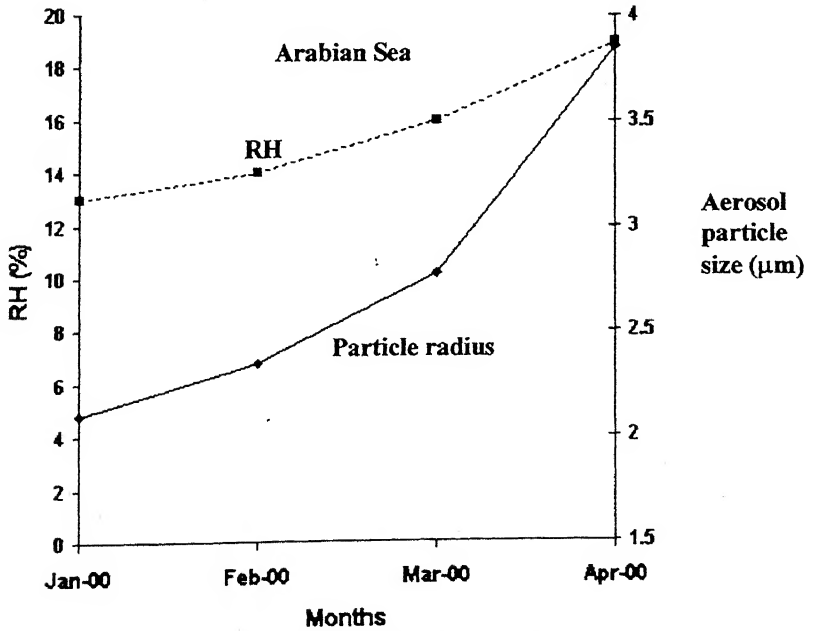

Fig. 5.8 Relative humidity and aerosol particle size near the coast

The relative humidity data has been taken from NCEP/NCAR. Fig. 5.8 shows that with increase in relative humidity, aerosol particle size also increases. Fig. 5.9 shows the effect of relative humidity on the aerosol particle size over the remote ocean.

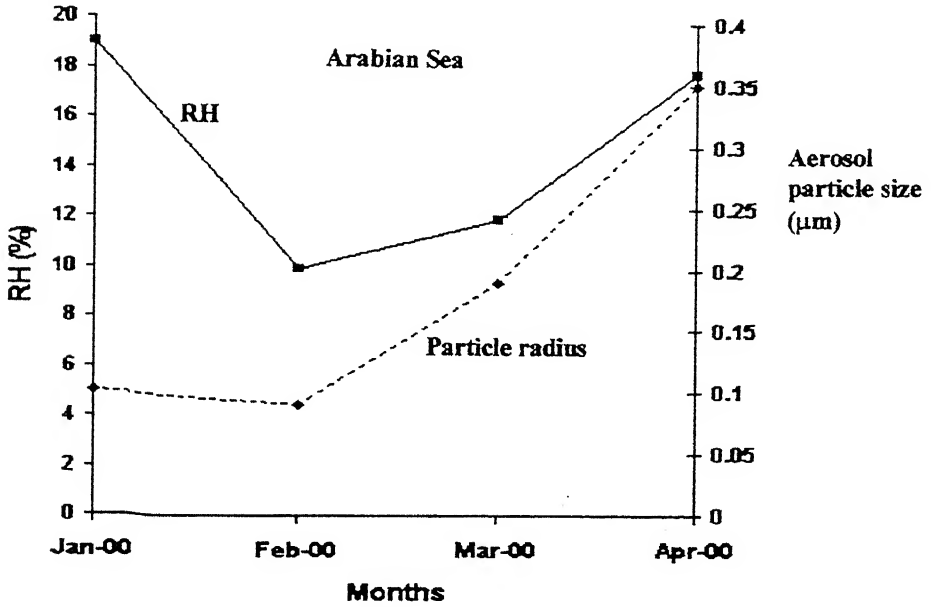

Fig. 5.9 Relative humidity and aerosol particle size in the remote ocean

Fig. 5.9 also shows similar effect occurring over the remote ocean. As the relative humidity decreases in the month of February from January 2000, the aerosol particle size is found to decrease. It increases during March and April 2000. However, the increase of the aerosol particle size is not solely attributed to the increase in relative humidity. During summer, evaporation from the land and ocean increases, which contributes to the higher water vapor in the atmosphere. The increased water vapor content in the atmosphere contributes to the growth of the already nucleated aerosol particles.

Three types of aerosols have been found over the Bay of Bengal. Fig. 5.10 shows the temporal variations of the three types of aerosols. The particles with the lowest value are background aerosols, which show no change, whereas, the other two types of aerosols show variation from November 1999 to May 2000. The highest particle size is for coastal aerosols, which is likely transported from the continent. The other type of aerosol is typically marine in nature. The coastal aerosol particles show larger variations compared those of marine aerosols.

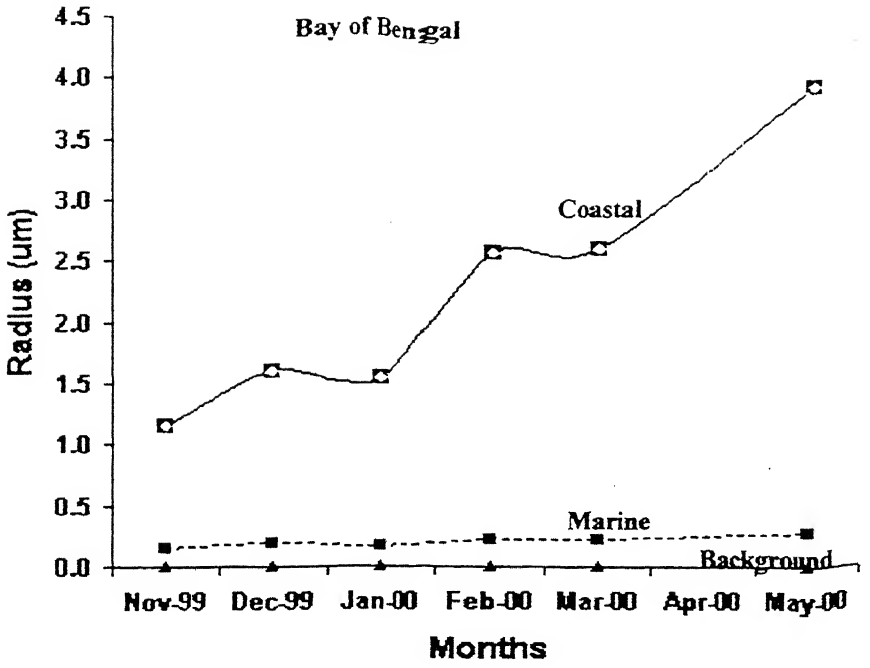

Fig. 5.10 Aerosol particle size over the Bay of Bengal

The particle size of the coastal and marine aerosol decreases during January and increase during other months with the highest value achieved during May 2000. This pattern of variations has been studied in view with the relative humidity in the atmosphere. Figs. 5.11 and 5.12 show the effect of relative humidity on the particle size of the coastal and marine aerosols.

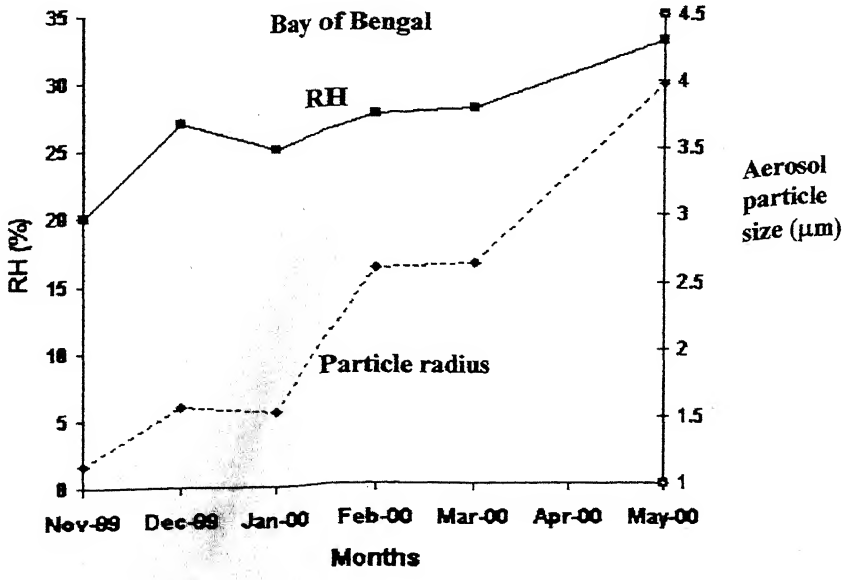

Fig. 5.11 Relative humidity and aerosol particle size near the coast

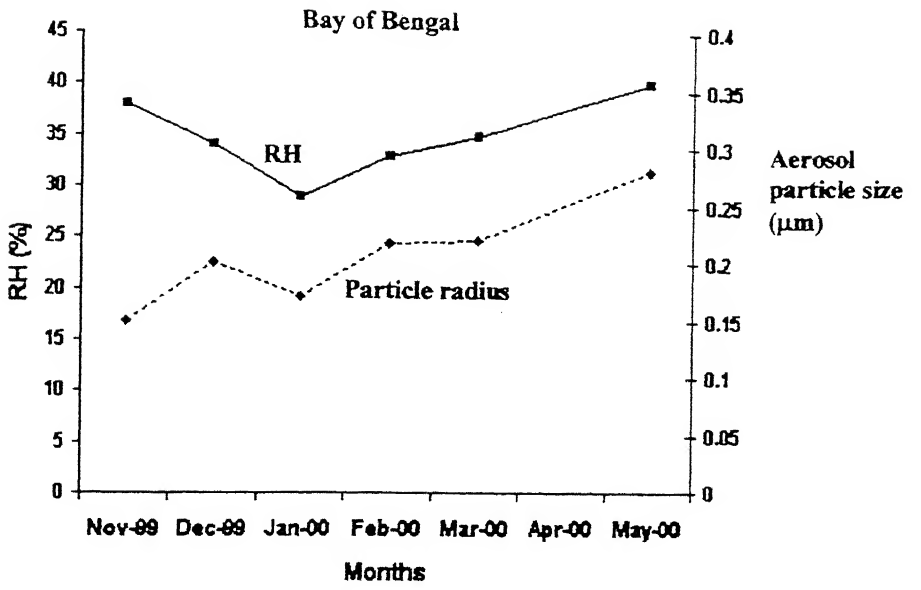

Fig. 5.12 Relative humidity and aerosol particle size in the remote

The effect of the relative humidity on the coastal aerosol particles over the Bay of Bengal is similar to that of the Arabian Sea. However, in the remote ocean, this effect is not seen during December. This behavior can be explained by the high wind speed in this region during this period. It has been found that during the month of December, the wind direction is towards the remote ocean (Fig. 5.14), which carries the coastal aerosols to the remote ocean. As a result, the residence time of the coastal aerosols in the month of December decreases, whereas, that for the marine aerosols increases (Fig. 5.15). In the size range under consideration basically two aerosol production mechanisms are operative. These are gas-to-particle and bulk-to-particle conversion (Jaenicke 1984). The former process is effective mainly for the submicron size i.e. in the remote ocean, whereas, the latter is effective for larger sizes i.e. in the coastal region.

The wind speed (Fig. 5.13) and the wind direction (Fig. 5.14) over the Arabian Sea and the Bay of Bengal has been deduced using QuikSCAT data.

16 NOV., 1999

10 DEC., 1999

2 JAN., 2000

21 JAN., 2000

3 FEB., 2000

29 FEB., 2000

2 MAR., 2000

21 MAR., 2000

29 APR., 2000

28 MAY., 2000

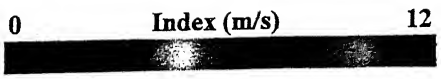

Fig. 5.13 Wind Speed over the Arabian Sea and the Bay of Bengal

16 NOV., 1999

10 DEC., 1999

2 JAN., 2000

21 JAN.. 2000

3 FEB., 2000

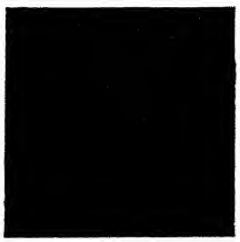

29 FEB., 2000

2 MAR., 2000

21 MAR., 2000

29 APR., 2000

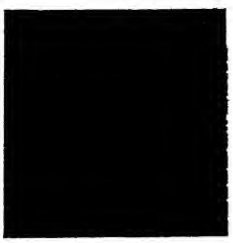

28 MAY, 2000

Fig. 5.14 Wind direction over the Arabian Sea and the Bay of Bengal

An important consideration for characterizing aerosol behavior is the understanding of the dynamic processes to specify the evolution of aerial suspension in time. The loss processes include collisional scavenging, diffusional transport and sedimentation fall out. Within the two competing processes of production and loss, aerosol particles in the atmosphere have a definite lifetime. Fig. 5.15 shows the variation of the aerosol residence time.

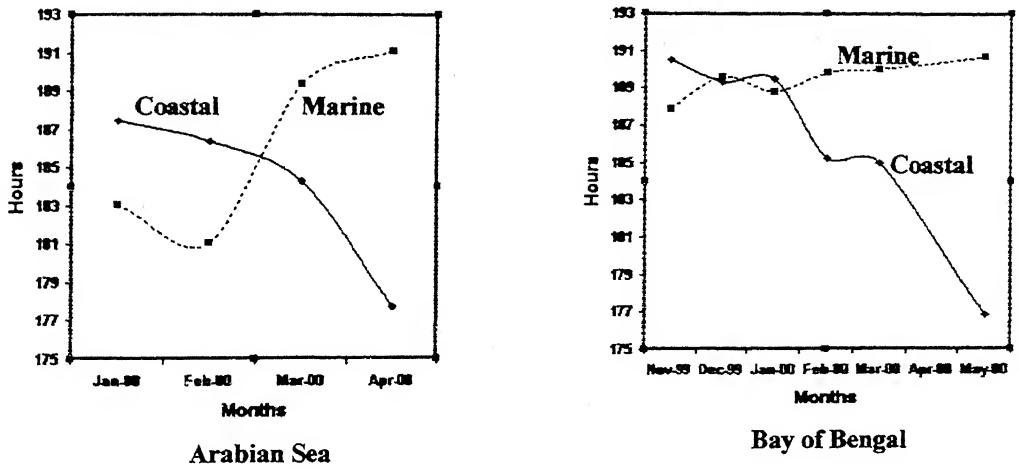

Fig. 5.15 Aerosol residence time over the Arabian Sea and the Bay of Bengal

The results show that the aerosol residence time over the Arabian Sea and the Bay of Bengal has similar behavior (Fig. 5.15). The aerosol residence time depends on two factors, aerosol particle size and wind speed. The residence time increases with the increase in wind speed and decrease in aerosol particle size. The residence time of the coastal aerosols decreases during the months January to April 2000 over the Arabian Sea and during the months November 1999 to May 2000 over the Bay of Bengal. The range varies from 177 to 187 hours for the coastal aerosols, whereas, it is 183 to 191 hours for marine aerosols over the Arabian Sea. The range over the Bay of Bengal varies within 176 to 191 hours for the coastal aerosols and 187 to 191 hours for marine aerosols. It is seen that before the month of March 2000, the residence time of the coastal aerosols over the Arabian Sea is higher compared to that for the marine aerosols, whereas, over the Bay of Bengal, the residence time for the coastal aerosols is higher compared to that for marine aerosols before the month of January 2000. Over the Arabian Sea, it is seen that near the coastal region, the wind speed decreases in the month of February and slightly increases in the months of March and April (Fig. 5.13). The increase of wind speed leads to the increase in the particle size in the months of March and April. Due to wind speed and particle size of the aerosols, the

residence time near the coastal region decreases. In the remote ocean, though the particle size increases, the variations are not large enough to have significant effect on the residence time. For marine aerosols, the wind speed plays the major role. During summer, the loss of aerosol is lower than the production of aerosols, due to enhanced evaporation. This leads to the increase in residence time. Over the Bay of Bengal, near the coast, the effect of the large particle size overshadows the effect of wind speed. With the increase in wind speed particle size also increases which leads to sharp decrease in aerosol residence time specially during months December 1999 and May 2000 (Fig. 5.15). Over the remote ocean, the variations of the residence time is not much due to marginal change in particle size. Though the wind speed increases during May, its effect is overbalanced by the increased rate of production of aerosols, thus ultimately resulting in small increase in residence time.

5.2 COLUMN WATER VAPOR

The column water vapor gives the total amount of total column water (TCW) vapor present in the atmosphere at a particular time. Column water vapor has been derived over the Arabian Sea and the Bay of Bengal and also over the adjacent land region. Fig. 5.16 shows the spatial and temporal variations of total column water vapor over the Arabian Sea and the adjacent land region. The monthly variations of total column water vapor (TCW) show characteristic behaviour over Indian land and ocean regions. The amount of water vapor in the atmosphere is indicative of the clima5tic and meteorological conditions of the region. The value of TCW over the ocean during the winter season is low compared to that during the summer season. A phase transition occurs from liquid to vapor in summer season due to intense heat, which gives a higher TCW value over the ocean.

JAN., 2000

65E, 25N

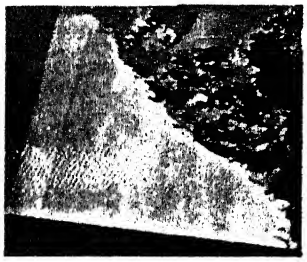

67E, 31N

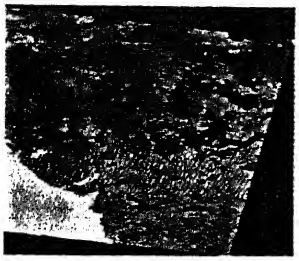

73E, 18N

81E, 17N

FEB., 2000

65E, 25N

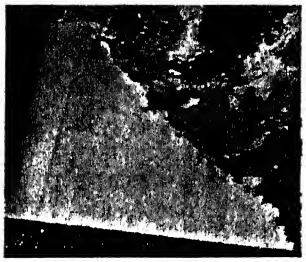

67E, 31N

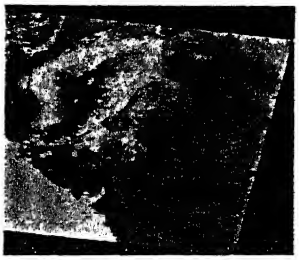

73E, 18N

81E, 17N

MAR., 2000

65E, 25N

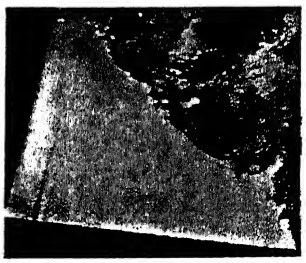

67E, 31N

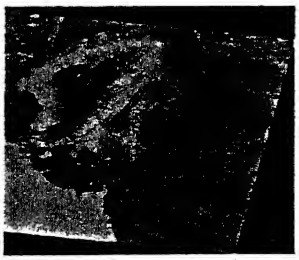

73E, 18N

81E, 17N

APR., 2000

65E, 25N

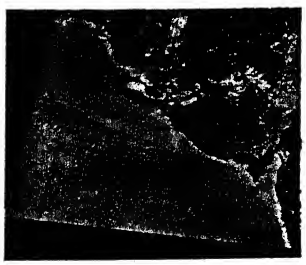

67E, 31N

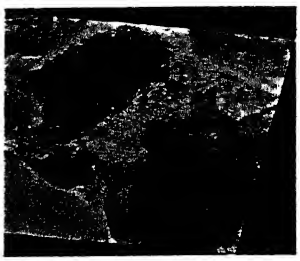

73E, 18N

81E, 17N

Ocean

Land

0 Index (mm) >70

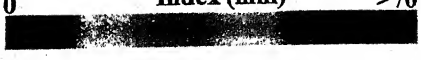

Fig. 5.16 Total column water vapor over the Arabian Sea and adjacent land region

The seasonal variations of TCW show characteristic behavior over the Arabian Sea and the adjacent land. From January to April, the TCW over the Arabian Sea varies from 25-55 mm, with higher value of > 55 mm in the bay region. During April, the maximum TCW is seen in the range 65-85 mm over the Thar Desert and the surrounding area. Over the land, TCW increases from January to April. TCW over the ocean is found to be low compared to that over the land. Variations of TCW over the Arabian Sea is seen during January to March, which shows a systematic pattern, whereas, during April, the pattern is not seen (Fig. 5.16). The direction of the systematic pattern varies in the northwest-southeast direction. The Thar Desert lies in the western India in Rajasthan. During summer, the surface and air temperature in the lower troposphere over the Thar Desert is higher, resulting in higher water holding capacity and hence higher TCW. During January to March, the circulation over the land is controlled by the mid-latitude easterly flow and associated cloudiness. The prevailing air-current is comparatively drier in the lower troposphere and as a result the TCW is moderately distributed over the land other than the Thar Desert. The higher and moderate TCW are likely to be attributed to higher evaporation from the surface and the transport of the water vapor in the region from the adjacent Arabian Sea.

Fig. 5.17 shows the spatial and temporal variations of TCW over the Bay of Bengal and the adjacent land. TCW over the Bay of Bengal shows systematic pattern like the Arabian Sea (Fig. 5.17). During November to May, TCW over the Bay of Bengal shows highest value (70 mm) in the month of January especially in the central part. Generally, TCW varies between 15 to 60 mm over the ocean. The systematic pattern of TCW varies in east-west direction during December and January. This trend changes during February to May, to the northwest-southeast direction. Variations of TCW over the Bay of Bengal show higher value over remote ocean compared to the coastal region. The coastal region generally contains large amount of suspended sediments, as a result the evaporation may decrease. Over the adjacent land region, TCW is found in the range 10 to 70 mm, with maximum values during summer. During summer, higher evaporation from land is likely, which leads to higher value of TCW. The increase in TCW during summer is also attributed to the onset of monsoon.

NOV., 1999

74E, 19N

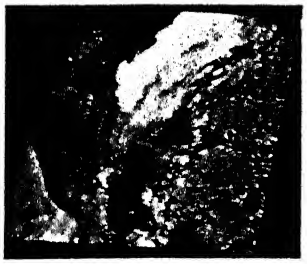

91E, 5N

74E, 19N

84E, 8N

DEC., 1999

74E, 19N

91E, 5N

74E, 19N

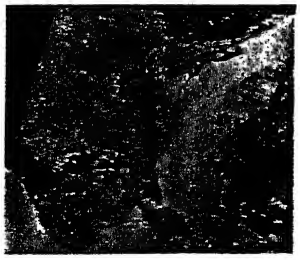

84E, 8N

JAN., 2000

74E, 19N

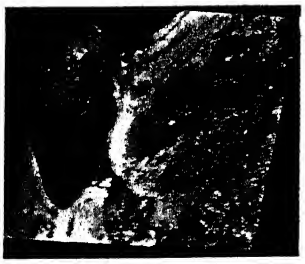

91E, 5N

74E, 19N

84E, 8N

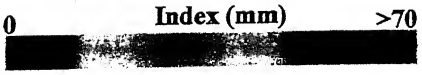

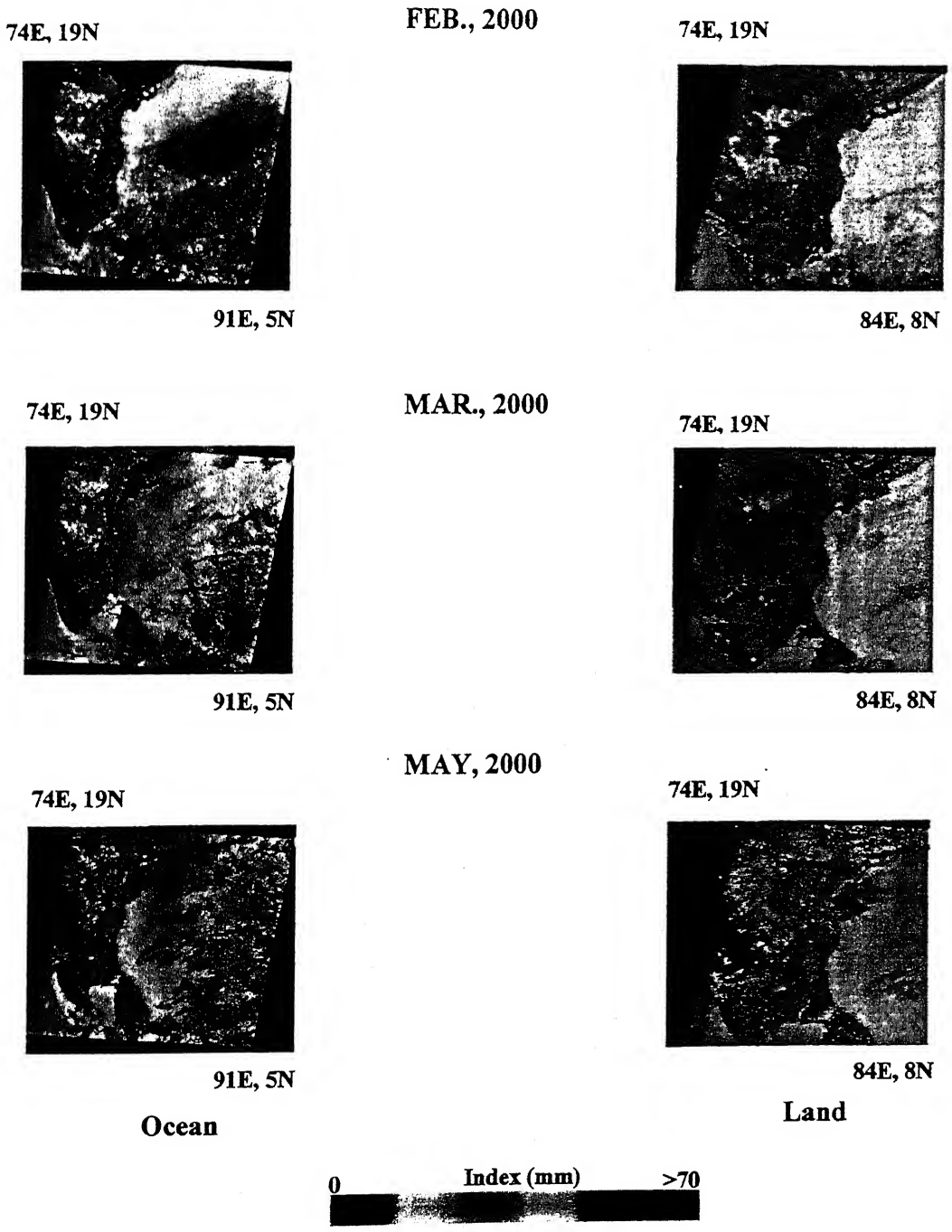

Fig. 5.17 Total Column Water Vapor over the Bay of Bengal and the adjacent land region

The amount of water vapor in the atmosphere is indicative of the climatic and meteorological conditions of the region. The systematic pattern of the spatial and temporal variations of TCW over the Arabian Sea and the Bay of Bengal is related to southwest and northeast monsoon (Fig. 5.16 and Fig. 5.17). The TCW variations over the ocean tend to move from higher latitude to lower latitude. Prior to monsoon, a cyclonic vortex is developed over the Arabian Sea. This increases the intensity of monsoonal flow and carries large amount of water vapor from the Southern Hemisphere (Krishnamurti, 1985). It is also interesting to note that prior to monsoon, the TCW is highest along the Arabian coast. The inter-annual variation of TCW and the change in its pattern is closely related to the onset of the monsoon and the dynamics of the climatic conditions.

Fig. 5.18 shows the water vapor content in the atmosphere over the land region measured at IIT Kanpur by sun photometer.

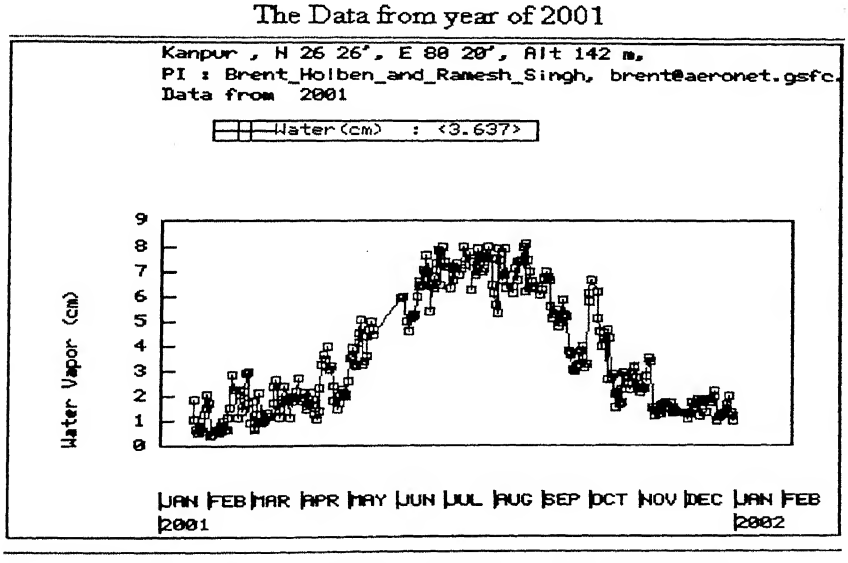

Fig. 5.18 TCW in the atmosphere in Kanpur

The water vapor measured at IIT Kanpur shows higher water vapor content during summer in the range 50 to 70 mm. The TCW deduced from OCM data over the land shows similar behavior and the amount measured by sun photometer at IIT Kanpur.

5.3 OCEANIC PARAMETERS

5.3.1 CHLOROPHYLL CONCENTRATION

Chlorophyll concentration has been retrieved over the Arabian Sea and the Bay of Bengal, which is shown in Figs. 5.19 and 5.20.

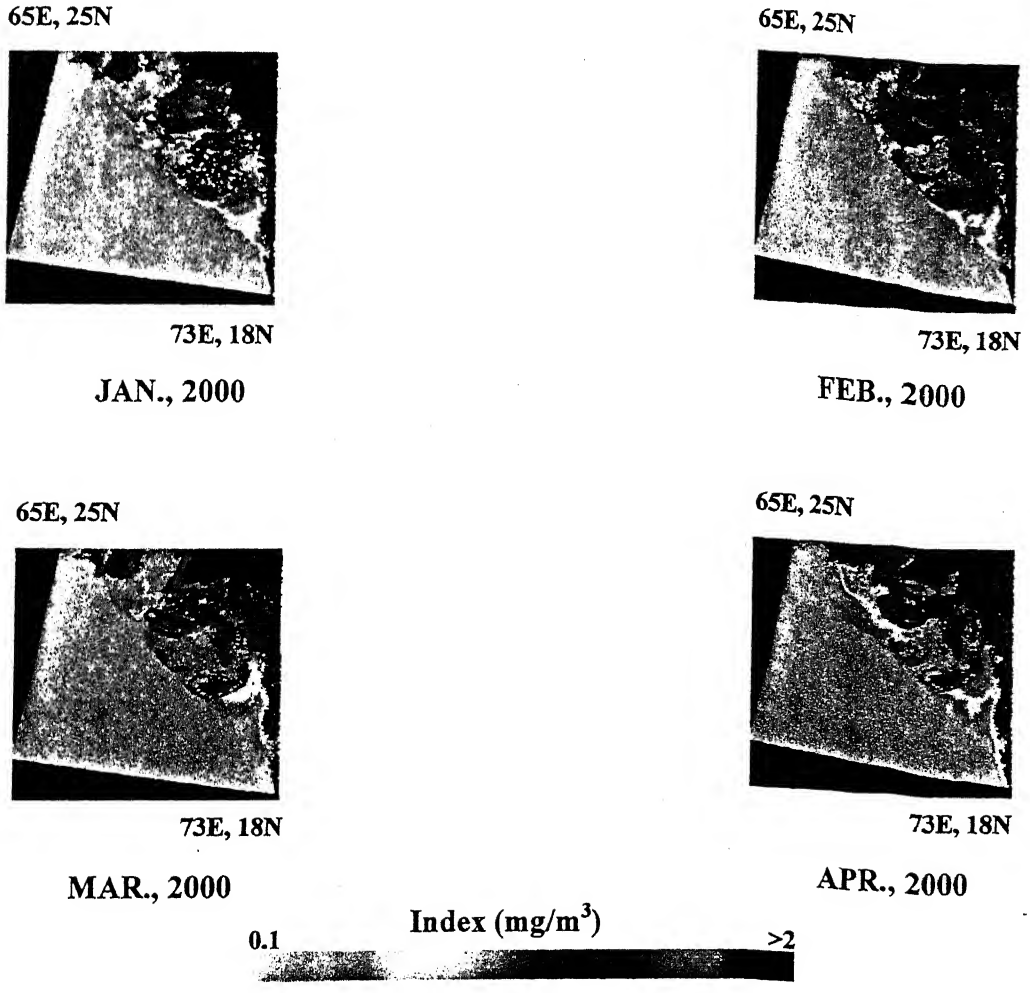

Fig. 5.19 Chlorophyll concentration in the Arabian Sea

Chlorophyll concentration in the Arabian Sea varies from 0.1 to >2 mg/m^3 (Fig. 5.19). The value is as low as 0.1 to 0.5 mg/m^3 in the remote ocean for all the months and shows higher value near the coastal areas. The two gulf areas, Gulf of Cambay and the Gulf of Kutch show maximum values in the range 1 to >2 mg/m^3. There are insignificant variations of chlorophyll concentration in the remote ocean. Near the coastal region, maximum chlorophyll concentration is seen in the month of January 2000 and it decreases in February and March, again increases marginally in April

2000 (Fig. 5.19). During winter, due to monsoonal flow, the land region suffer precipitation, as a result, the westerly flowing rivers carry nutrients to the ocean. This leads to the increase in chlorophyll bloom during winter. Afterwards, due to decrease in nutrients, chlorophyll concentration decreases. Chlorophyll concentration, an index of phytoplankton biomass, is the single most important property of marine ecosystem. In the Arabian Sea, most of the primary production occurred below the surface during the northeast monsoon from October to January and the value is higher than during premonsoon.

Chlorophyll concentration in the Bay of Bengal varies from 0.1 to <2 mg/m^3 (Fig. 5.20). The chlorophyll concentration is low in the remote ocean and shows almost no variation through out the seasons. The value is higher near the coastal region with the highest value is observed near the Godavari and Krishna delta. The high chlorophyll concentration in the coastal region is attributed to higher availability of nutrients along the coast. The nutrients are carried by rivers from continent and also are supplied by upwelling resulting from vertical mixing. The higher value of chlorophyll concentration is observed during winter, which is due to high precipitation in the land region by winter monsoon and subsequently higher nutrient transport to the ocean. Chlorophyll concentration is found to be higher in the Arabian Sea compared to the Bay of Bengal.

74E, 19N

91E, 5N

NOV., 1999

74E, 19N

91E, 5N

DEC., 1999

74E, 19N

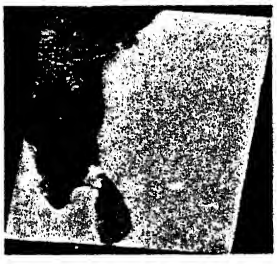

91E, 5N

JAN., 2000

74E, 19N

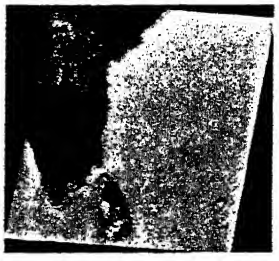

91E, 5N

FEB., 2000

74E, 19N

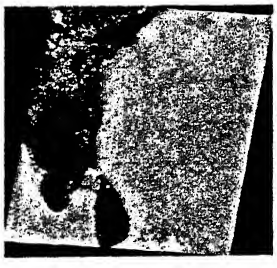

91E. 5N

MAR., 2000

74E, 19N

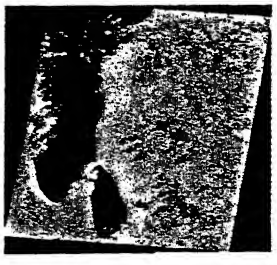

91E. 5N

MAY, 2000

Index (mg/m^3)

0.1 >2

Fig. 5.20 Chlorophyll concentration in the Bay of Bengal

5.3.2 SUSPENDED SEDIMENT CONCENTRATION

Suspended sediment concentration is another oceanic parameter, which is deduced from the OCM data. Fig. 5.21 shows the suspended sediment concentration in the Arabian Sea during January to April 2000.

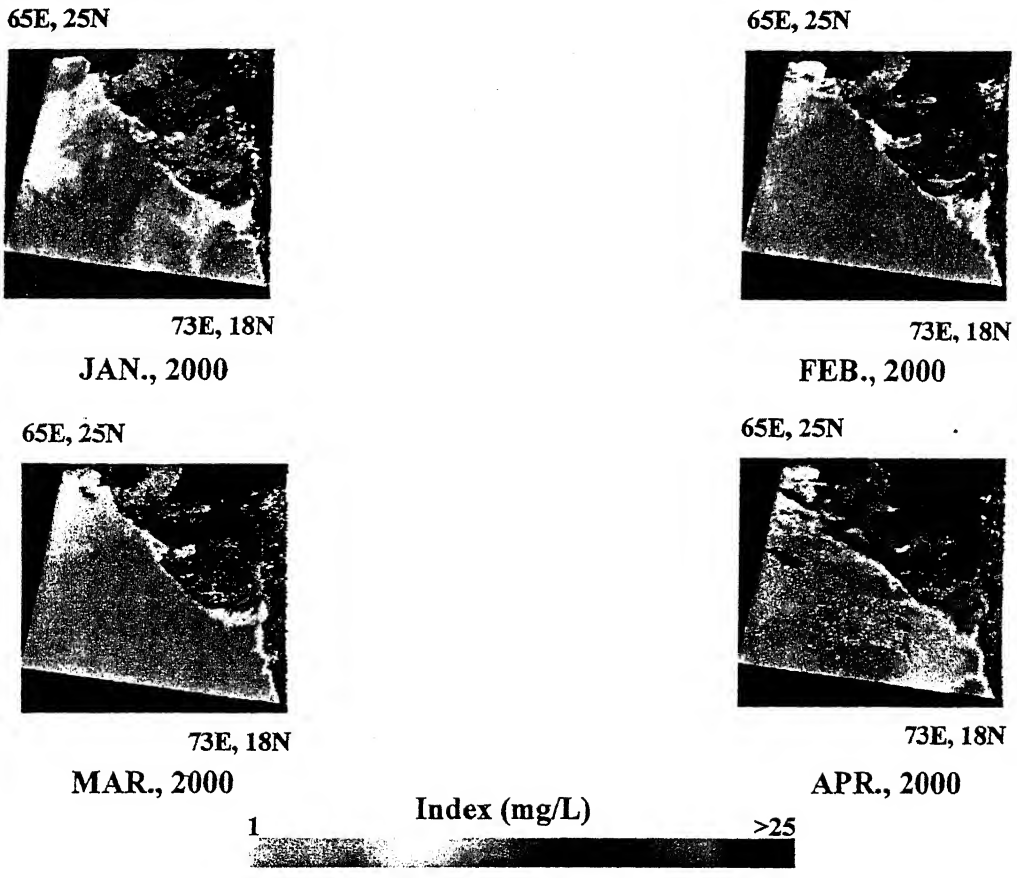

Fig. 5.21 Suspended sediment concentration in the Arabian Sea

The results show that the suspended sediment concentration in the Arabian Sea varies in the range of 1 to 30 mg/L (Fig. 5.21). Higher value is observed near the coastal region with the maximum value of > 25 mg/L in the Gulf of Cambay and in the northwestern Arabian Sea. The two main rivers Narmada and Mahi flow into the Arabian Sea in the Gulf of Cambay and the Indus flows into the northwestern Arabian Sea. The higher value of suspended sediment concentration in this region is attributed to the transport of huge sediments throughout the year by these rivers. Higher value of suspended sediment concentration is observed in the month of April compared to the other months with the lowest value observed in February.

Fig. 5.22 shows the suspended sediment concentration in the Bay of Bengal.

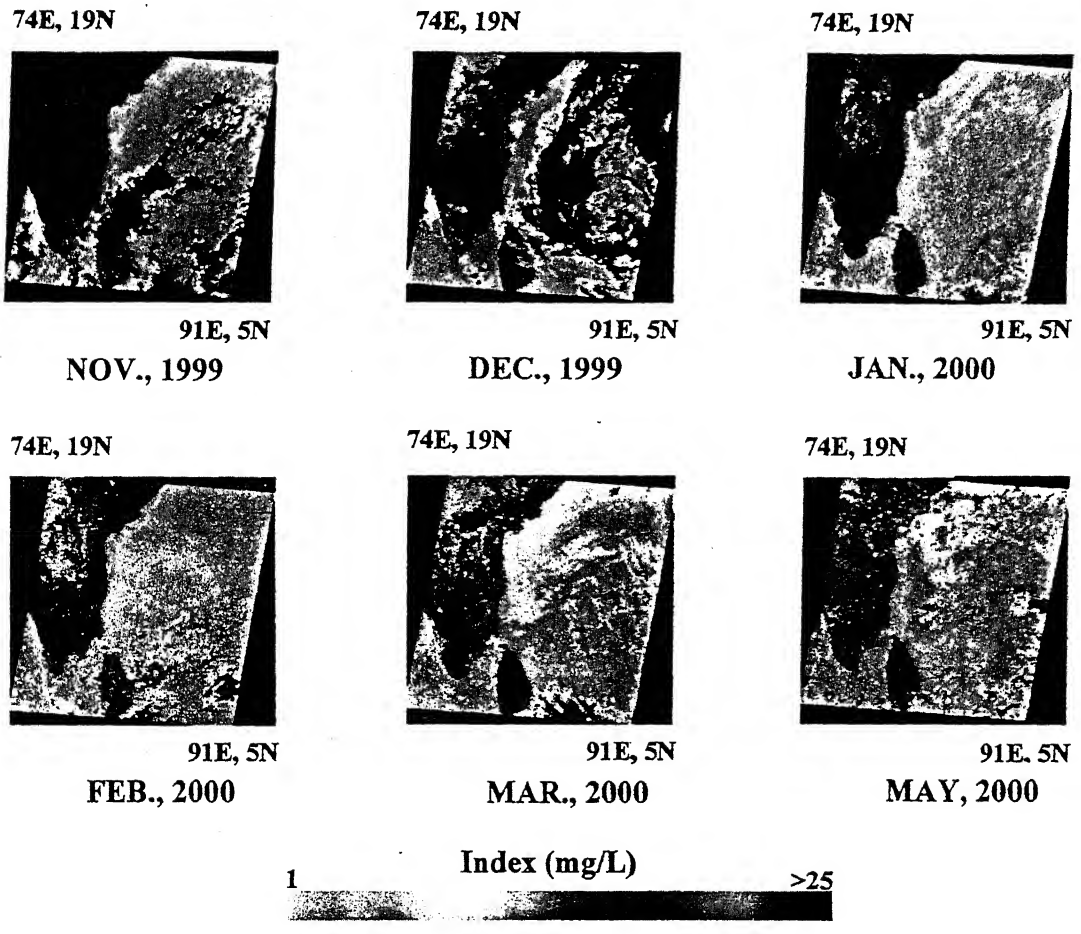

Fig. 5.22 Suspended sediment concentration in the Bay of Bengal

Suspended sediment concentration in the Bay of Bengal also shows higher value in the coastal region, with the highest value of >25 mg/L in the Godavari and Krishna delta (Fig. 5.22). The suspended sediment concentration in the remote ocean shows almost no variation throughout the seasons. Higher value is observed in the month of January, which is attributed to the higher input of sediments by easterly flowing rivers during precipitation in the months of November to January. Higher value of suspended sediment concentration is found in the Arabian Sea compared to the Bay of Bengal.

CHAPTER VI
CONCLUSIONS

5.0 SUMMARY AND CONCLUSION

In the present work, efforts have been made to deduce atmospheric and oceanic parameters over the Arabian Sea and the Bay of Bengal and the adjacent land region during the months November 1999 to May 2000 from OCM data. The algorithms used in this present study have been validated by the researchers in SAC, ISRO, Ahmedabad. The following conclusions can be drawn from the present study.

- AOD has been retrieved at wavelengths 765 and 865 nm and in the bay region, which has been corrected for turbidity. It has been found that AOD at wavelength 765 nm is higher compared to those at 865 nm. Due to turbidity, AOD has been over-estimated.
- AOD is found to be higher during summer compared to that during winter over the Arabian Sea and the Bay of Bengal. The spatial gradient of AOD over the Bay of Bengal is found to be higher compared to that over the Arabian Sea.
- Three types of aerosol particles have been found over the Arabian Sea and the Bay of Bengal. Coastal aerosols are larger in size (>1 μm). Marine aerosols are in medium size range (0.1 to 0.4 μm) and the background aerosols are very small (0.001 to 0.004 μm).
- Aerosol particles are found to increase in size during summer and the change in the aerosol particle size has been correlated with the relative humidity in the atmosphere.
- Residence time of the coastal aerosols is found to decrease during summer, whereas, in the remote ocean it is found to increase. In the coastal region, the residence time of the aerosols are mainly dominated by their particle sizes, whereas, in the remote ocean, wind speed and wind direction play the major role.
- Water vapor over the ocean and the adjacent land region has been deduced. Higher evaporation during summer leads to higher water vapor in the atmosphere during summer.
- Water vapor over the ocean is found to be lower compared to that over the land. The value of the water vapor content in the atmosphere over the land has been

compared with the value measured by the sun photometer and it has been found that the value deduced from the remotely sensed data are well in tandem with the ground measurements.

- Chlorophyll and suspended sediment concentrations have been deduced in the Arabian Sea and the Bay of Bengal. High chlorophyll concentration has been found in the Arabian Sea compared to that in the Bay of Bengal. Chlorophyll concentration has been found to be higher during winter compared to that during summer. This is attributed to the higher nutrient supply by rivers from continent during northeast monsoon and by upwelling through vertical mixing.
- Higher suspended sediment concentration has been found in the bay region in the Arabian Sea and the Bay of Bengal, which is attributed to the transport of sediments by some major rivers from the Indian subcontinent.

6.1 LIMITATIONS OF THE WORK

- The standard algorithms have been used to retrieve the chlorophyll and suspended sediment concentration, not taking into account the details of the local effect.
- The parameters over the Arabian Sea and the Bay of Bengal have not been validated by ground measurements, as the ground measurements over the ocean are difficult to perform.

6.2 FUTURE RECOMMENDATIONS

Based on the present study, the future recommendations that can be made are:

- Ground based measurements should be taken to validate the results to have proper correlation of the remotely sensed data with the actual data
- Model based approaches can be taken to generate new algorithms, which can deal with the local effects.

REFERENCES

C. E. Junge (1963): Air chemistry and Radioactivity. Academic Press, pp. 382.

C. E. Junge, (1972): Our knowledge of the physico-chemistry of aerosols in the undisturbed marine environment. Journal of Geophysical Research 77, pp. 5183-5200.

Chandra Venkataraman, Anurag Mehra and Prashant Mhaskar (2001): Mechanisms of sulphate aerosol production in cloud characteristics and Season in the Indian region. Tellus, 53B, 260-272.

D. C. Blanchard, A H. Woodcock, (1980): The production, concentration and vertical distribution of the Sea-salt aerosols. Ann. Of the N. Y. Academy of Sciences 338, pp. 330-347.

Dan Ling Tang and Hiroshi Kawamura (2001): Remote sensing on the Asian waters: Ocean color products of high spatial resolution and long-term series. Proceedings of the Eleventh, PAMS/JECSS Workshop, April 11-13, 2001, Cheju, Korea.

Dan Ling Tang, I-Hsun Ni, Dana R. Kester and Frank E. Muller-Karger (1999): Remote sensing observations of winter phytoplankton blooms southwest of the Luzon strait in the South China Sea. Marine ecology progress series, Vol. 191, pp. 43-51, 1999.

E. C. Monahan, D. E. Spiel, K. L. Davidson (1986): A model of marine aerosol generation via white caps and wave disruption. Q. J. R. Meterol. Soc.

G. P. Box, M. A. Box and A. Deepak (1981): On the spectral sensitivity of the approximate method for retrieving aerosol size distribution from multispectral solar extinction measurements. J. Appl. Meteor., 20, pp. 944-948.

H. R. Gordon (1997): Atmospheric correction of ocean color imagery in the Earth Observing System era. Journal of Geophysical Research, 102, pp. 17081-17106.

Indian Remote Sensing Satellite IRS-P4 (OCEANSAT) Handbook (1999). Payloads orbits and coverages, National Remote Sensing Agency, Department of Space, Government of India, Hyderabad.

J. E. O'Reilley, Maritorena, B. G. Mitchell, D. A. Siegal, K. L. Carder, S. A. Kahru and C. R. McClain (1998): Ocean color chlorophyll algorithms for SeaWiFS. Journal of Geophysical Research, Vol. 103, pp. 24937-24953.

K. Krishna Moorthy, Prabha R. Nair and B. V. Krishna Murthy (1990): Size distribution of coastal aerosols: Effects of local sources and sinks. Journal of Applied Meteorology, Vol. 30, pp. 844-852.

K. Krishna Moorthy, Preetha S. Pillai, Auromeet Saha and K. Niranjan (1999): Aerosol size characteristics over the Arabian Sea and Indian Ocean: Extensive sub-micron aerosol loading in the Northern Hemisphere. Current Science, Vol. 76, No. 7, April 1999.

K. Krishna Moorthy, S. K. Sathesh and B. V. Krishna Murthy (1998): Characteristics of spectral optical depths and size distributions of aerosols over tropical oceanic regions. Journal of Atmospheric and Solar-Terrestrial Physics 60 (1998), pp. 981-992.

K. Niranjan, S. Thulasiraman, G. V. Satyanarayana, and Y. Ramesh Babu (2000): Temporal Characteristics of Aerosol optical depths and Size Distribution at Visakhapatnam, India. Aerosol Science and Technology, American Association for Aerosol Research (in press).

K. Parameshwaran (1998): Atmospheric aerosols and their radiative effects. PINSA, 64, A, No. 3, May 1998, pp. 245-266.

K. Parameswaram and G. Vijayakumar (1994): effect of relative humidity on aerosol size distribution. Indian Journal of Radio & Space Physics, Vol. 23, June 1994, pp. 175-188.

K. Rajeev, V. Ramanathan and J. Merywerk (2000): Regional aerosol distribution and its long-range transport over the India Ocean. Journal of Geophysical Research, Vol. 105, No. D2, pp. 2029-2043, 2000.

L. M.Russell, S. N. Pandis, J. H. Seinfeld (1994): Aerosol production and growth in marine boundary layer. Journal of Geophysical Research 99, 20.989-21.003.

M. G. Lawrence, (1993): An emperical analysis of the strength of the phytoplankton-dimethylsulfide-cloud-climate feedback cycle. Journal of Geophysical Research 98.20, pp. 663-673.

M. Mohan (2000): Atmospheric correction for ocean color remote sensing and detection of atmospheric aerosols. Pre-conference training, 1-5, Goa, India, Dec. 1-4, 2000.

P. Schlussel and W. J. Emery (1990): Atmospheric water vapor over oceans from SSM/I measurements. International Journal of Remote Sensing, Vol. 11, pp. 5753-5766.

Prakash Chauhan (2000): Retrieval of water constituents using ocean color data: IRS-P4 OCM data processing. Pre-conference training, 1-5, Goa, India, Dec. 1-4, 2000.

R. Bennartz and J. Fischer (1998): Retrieval of columnar water vapor over land from MOS and MERIS. Proceedings of 2nd International Workshop on MOS-IRS and Ocean Color, pp. 313-318, DLR, Berlin.

R. Doerffer (1992): Imaging spectroscopy for detection of chlorophyll and suspended matter. GKSS 92/E/54, GKSS-FORSCHUNGSZENTRUM GEESTHACHT GMBH.

R. Jaenicke (1984): Physical aspects of the atmospheric aerosol. Aerosols and their climatic effects. H. E. Gerber and A. Deepak, Eds., A. Deepak Publishing, pp.7

R. J. Charlson, J. E. Lovelock, M. O. Andrea, and S. G. Warren, (1987): Oceanic phytoplankton, atmospheric sulfur, cloud albedo and climate, Nature 326, pp. 655-661.

R. P. Singh, N. C. Mishra, A. Verma and J. Ramaprasad (2000): Total precipitable water over the Arabian Ocean and the Bay of Bengal using SSM/I data. International Journal of Remote Sensing, 2000, Vol. 21, No. 12, pp. 2497-2503.

S. Nakamoto, S. Prasanna Kumar, J. M. Oberhuber, K. Muneyama and R. Frouin (2000): Chlorophyll modulation of Sea surface tempearture in the Arabian Sea in a mixed layer isopycnal general circulation model. Geophysical research Letters, Vol. 27, No. 6, pp. 747-750, March 15, 2000.

S. Tahl and M. V. Schonermark (1998): Determination of the column water vapor of the atmosphere using backscattered solar radiation measured by the Modular Optoelectronic Scanner (MOS). International Journal of Remote Sensing, No. 17, Vol. 19, pp. 3223-3236.

S. Tassan and B. Strum (1986): An algorithm for the retrieval of sediment content and turbid coastal waters from CZCS data. International Journal of Rmote Sensing, Vol. 7, pp. 643-655.

Yasuhiko Okada, Sonyo Mukai and Itaru Sano (2002): A new algorithm to retrieve aerosol over the Gulf of Cambay in India. International Journal of Remote Sensing (submitted).